QUALITY INFORMATION DOCUMENT

For Global Sea Physical Analysis and Forecasting Product

GLOBAL_ANALYSIS_FORECAST_PHY_001_024

Issue: 2.0

Contributors :J-M. LELLOUCHE, O. LEGALLOUDEC, C.REGNIER, B. LEVIER, E. GREINER,M.DREVILLON

Approval Date by Quality Assurance Review Group : October 2016

CHANGE RECORD

Issue	Date	§	Description of Change	Author	Validated By
1.0	23/09/2016	All	Creation of the document for CMEMS V2.3	M. Drevillon	Y. Drillet
2.0	19/10/2016		Correction after review	J. M. Lellouche	Y. Drillet

TABLE OF CONTENTS

I EXECUTIVE SUMMARY

I.1 Products covered by this document

The products assessed in this document are referenced as:

GLOBAL_ANALYSIS_FORECAST_PHY_001_024 for the physical 14-day hindcast (analyses, updated weekly), and for the physical 10-day forecast (updated daily). These products, hereafter referred to as GLO_HR products, contain global nominal fields on global standard grid in 1/12° (0.0833 ° lat x 0.0833° lon) with 50 geopotential levels from 0 to 5000m, for the following variables:

* sea_ice_area_fraction
* sea_ice_thickness
* eastward_sea_ice_velocity
* northward_sea_ice_velocity
* sea_surface_height_above_geoid
* sea_water_potential_temperature_at_sea_floor
* ocean_mixed_layer_thickness_defined_by_sigma_theta
* sea_water_potential_temperature
* sea_water_salinity
* eastward_sea_water_velocity
* northward_sea_water_velocity

Note that two different datasets are available:

- global-analysis-forecast-phys-001-024

  containing 3D daily means
- global-analysis-forecast-phys-001-024-hourly-t-u-v-ssh

  containing surface hourly outputs

I.2 Executive summary

The quality of the Global high resolution system and GLO_HR products has been assessed using one year of the hindcast. The headline results for each of the variables assessed are as follows.

I.2.1 Temperature and salinity

The systems description of the ocean water masses is very accurate on average and departures from in situ observations rarely exceed 0.5 K and 0.1 psu. In the thermocline, RMS errors reach 1 K and 0.2

psu. In high variability regions like the Gulf Stream or the Agulhas Current, or the Eastern Tropical Pacific, RMS errors reach more than 2 K and 0.5 psu locally.

A warm bias persists in subsurface, with peaks in high variability regions such as the Eastern Tropical Pacific Gulf Stream or Zapiola. Near the surface, these biases compensate on average with cold biases in the mean latitude, which reach a peak during boreal summer. A fresh bias still occurs near the surface mostly in tropical regions. Deep biases may develop in the systems and have to be investigated further and better monitored.

I.2.2 SST

A warm SST bias of 0.1 K on average is observed in the V2.3 global products. In summer, the global average warm bias partly compensates with a cold surface bias in the mid-latitudes, which seems to be due to a lack of stratification in summer. Vertical physics have to be improved in future versions of the system.

I.2.3 SLA

The GLO_HR products are generally very close to altimetric observations (global average is below 6cm RMS error).

The GLO system assimilates along track observations from all altimetric missions available from the CMEMS Sea Level TAC. The correlation of GLO_HR hourly SSH products with tide gauges is significant at all frequencies, however many high frequency fluctuations of the SSH might not be captured by the GLO_HR products (note that tides or pressure effects are not modelled).

I.2.4 Ocean currents

Surface currents of the mid latitudes are underestimated on average with respect to in situ measurements of drifting buoys. The underestimation ranges from 20% in strong currents to 60% in weak currents. Some equatorial currents are overestimated, and the western tropical Pacific still suffer from biases in surface currents related to MDT biases. On the contrary the orientation of the current vectors is better represented.

Due to the lack of high frequency current measurements at the global scale, the added value of the hourly surface currents has not been quantified yet. However, as the surface forcing is updated every 3 hours, the high frequency surface currents are expected to be relevant.

I.2.5 Sea Ice

The sea ice concentrations are overestimated in the Arctic mainly during winter (due to atmospheric forcings errors and too much sea ice accumulation). Sea ice concentration is overestimated in the Antarctic during austral winter (also due to atmospheric forcing errors) and underestimated during austral summer (too much sea ice melt and errors caused by the rheology parameterization of the sea ice model). The system does not capture well rapid fluctuations in sea ice cover, especially at the beginning of the melting season.

I.3 Estimated Accuracy Numbers

The following 3D T and S, SLA and SST **accuracy numbers** are an estimate **based on statistics performed at the time locations of the available observations**.

In all cases these numbers are an estimate of the likely error in most sub-regions of one given zone (NAT, TAT, MED, etc…) and not a maximum error on the zone.

Here are presented only the **accuracy numbers for the global area** (error statistics for each region are detailed in chapter III). Accuracy values are given by RMS and Mean errors for 3D Temperature; 3D salinity; for the following vertical layers: 0-5m, 5-100m, 100-300m, 300-800m, 800-2000m, 2000-5000m; and for SLA and SST. There is **no quantitative accuracy estimate for 3D ocean currents** in this document: further studies are necessary on the potential bias of near surface drifter observations and a general evaluation of surface currents is given in the summary.

In order to calculate these accuracy numbers we defined a one year **qualification (or calibration) period** in 2015. Results are presented following each variable.

I.3.1 Temperature

3D T (K) vs in situ Observations	Hindcast		Forecast day 3	
	Mean	RMS	Mean	RMS
0-5m	-0.03	0.65	tbc	tbc
5-100m	-0.05	0.89	tbc	tbc
100-300m	-0.06	0.78	tbc	tbc
300-800m	-0.03	0.43	tbc	tbc
800-2000m	0.00	0.17	tbc	tbc
2000-5000m	0.02	0.22	tbc	tbc
0-5000m	-0.01	0.41	tbc	tbc

Table 1: Global (GLO region) RMS and mean temperature misfits in K (observation-model) with respect to in situ observations (INS TAC), in contiguous layers from 0 to 5000m.

I.3.2 Salinity

3D S (PSU) vs in situ Observations	Hindcast		Forecast day 3	
	Mean	RMS	Mean	RMS
0-5m	0.005	0.199	tbc	tbc
5-100m	0.005	0.166	tbc	tbc

100-300m	-0.002	0.107	tbc	tbc
300-800m	0.000	0.057	tbc	tbc
800-2000m	0.001	0.026	tbc	tbc
2000-5000m	-0.003	0.017	tbc	tbc
0-5000m	0.000	0.061	tbc	tbc

Table 2: Global (GLO region) RMS and mean salinity misfits in psu (observation-model) with respect to the in situ observations (INS TAC), in contiguous layers from 0 to 5000m.

I.3.3 SST

SST (K) vs Satellite data	Hindcast		Forecast day 3	
	Mean	RMS	Mean	RMS
GLO	-0.1	0.45	tbc	tbc

Table 3: Global (GLO region) RMS and mean SST misfits in K (observation-model) with respect to observations (OSI TAC).

I.3.4 SLA

Seal Level Anomaly (cm) vs Satellite Along track data	Hindcast		Forecast day 3	
	Mean	RMS	Mean	RMS
GLO	0.63	5.50	tbc	tbc

Table 4: Global (GLO region) RMS and mean SLA misfits in cm (observation-model) with respect to altimetric along tracks observations (Sea Level TAC).

I.3.5 Sea Ice

Sea Ice Cover (%)	Hindcast		Forecast day 3	
	Mean	RMS	Mean	RMS
ARC	10%	20%	tbc	tbc
ACC	5%	25%	tbc	tbc

Table 5: ARC and ACC regions Mean and RMS misfist for Sea Ice Concentration (%) with respect to observations (OSI TAC).

II PRODUCTION SUBSYSTEM DESCRIPTION

These products are provided by Mercator Océan which is in charge of the GLO MFC production centre.

II.1 The physical high resolution (GLO_HR) global system

This system, called PSY4V3R1, produces:
– Global GLO_HR weekly 7-day hindcast, and nowcast.
– Global GLO_HR daily 10-day forecast.

The high resolution global analysis and forecasting system PSY4V3R1 uses version 3.1 of the NEMO ocean model (Madec et al., 2008). The physical configuration is based on the tripolar ORCA12 grid type (Madec and Imbard, 1996) with a horizontal resolution of 9 km at the equator, 7 km at Cape Hatteras (mid-latitudes) and 2 km toward the Ross and Weddell seas. The 50-level vertical discretization retained for this system has a decreasing resolution from 1m at the surface to 450 m at the bottom, and 22 levels within the upper 100 m. A "partial cells" parameterization (Adcroft et al., 1997) is chosen for a better representation of the topographic floor (Barnier et al., 2006) and the momentum advection term is computed with the energy and enstrophy conserving scheme proposed by Arakawa and Lamb (1981). The advection of the tracers (temperature and salinity) is computed with a total variance diminishing (TVD) advection scheme (Lévy et al., 2001; Cravatte et al., 2007). We use a free surface formulation. External gravity waves are filtered out using the Roullet and Madec (2000) approach. A laplacian lateral isopycnal diffusion on tracers and a horizontal biharmonic viscosity for momentum are used. In addition, the vertical mixing is parameterized according to a turbulent closure model (order 1.5 and mixing length of 30m) adapted by Blanke and Delecluse (1993), the lateral friction condition is a partial-slip condition with a regionalisation of a no-slip condition (over the Mediterranean Sea) and the Elastic-Viscous-Plastic rheology formulation for the LIM2 ice model (hereafter called LIM2_EVP, Fichefet and Maqueda, 1997) has been activated (Hunke and Dukowicz, 1997). Instead of being constant, the depth of light extinction is separated in Red-Green-Blue bands depending on the chlorophyll data distribution from mean monthly SeaWIFS climatology. The bathymetry used in the system is a combination of interpolated ETOPO1 (Amante and Eakins, 2009) and GEBCO8 (Becker et al., 2009) databases. ETOPO1 datasets are used in regions deeper than 300 m and GEBCO8 is used in regions shallower than 200 m with a linear interpolation in the 200 m – 300 m layer.). Internal-tide driven mixing is parameterized following Koch-Larrouy et al. (2008) for tidal mixing in the Indonesian Seas. The atmospheric fields forcing the ocean model are taken from the ECMWF (European Centre for Medium-Range Weather Forecasts) Integrated Forecast System. A 3 h sampling is used to reproduce the diurnal cycle. Momentum and heat turbulent surface fluxes are computed from the Large and Yeager (2009) bulk formulae using the following set of atmospheric variables: surface air temperature and surface humidity at a height of 2 m, mean sea level pressure and wind at a height of 10 m. Downward longwave and shortwave radiative fluxes and rainfall (solid + liquid) fluxes are also used in the surface heat and freshwater budgets. The estimation of Silva et al. (2006) is implemented in the system to represent the amount and distribution of meltwater which can be attributed to giant

and small icebergs calving from Antarctica, in the form of a monthly climatological runoff at the Southern Ocean surface. Lastly, the system does not include tides.

The data are assimilated by means of a reduced-order Kalman filter derived from a SEEK filter (Brasseur and Verron, 2006), with a 3-D multivariate modal decomposition of the forecast error and a 7-day assimilation cycle (Lellouche et al., 2013). It includes an adaptive-error estimate and a localization algorithm. The forecast error covariance is based on the statistics of a collection of 3-D ocean state anomalies, typically a few hundreds. This approach is based on the concept of statistical ensembles in which an ensemble of anomalies is representative of the error covariances. In this way, truncation no longer occurs and all that is needed is to generate the appropriate number of anomalies. This approach is similar to the Ensemble Optimal Interpolation developed by Oke et al. (2008). In our case, the anomalies are computed from a long numerical experiment (typically around 10 years) with respect to a running mean in order to estimate the 7-day scale error on the ocean state at a given period of the year. In addition, a 3D-Var scheme provides a correction for the slowly-evolving large-scale biases in temperature and salinity. Altimeter data, in situ temperature and salinity vertical profiles and satellite sea surface temperature are jointly assimilated to estimate the initial conditions for numerical ocean forecasting. Moreover, satellite sea ice concentration is now assimilated in the PSY4V3R1 system in a monovariate/monodata mode. In addition to the quality control performed by data producers, the system carries out two internal quality controls on temperature and salinity vertical profiles in order to minimise the risk of erroneous observed profiles being assimilated in the model.
The analysis is not performed at the end of the assimilation window but at the middle of the 7-day assimilation cycle. The objective is to take into account both past and future information and to provide the best estimate of the ocean centred in time. With such an approach, the analysis, to some extent, acts like a smoother algorithm. After each analysis, the data assimilation produces increments of barotropic height, sea surface height, temperature, salinity and zonal and meridional velocity. These increments are progressively applied using the Incremental Analysis Update (IAU) method (Bloom et al., 1996; Benkiran and Greiner, 2008) which makes it possible to avoid model shocks which happened every week due to the imbalance between the analysis increments and the model physics. In this way, the IAU reduces spin-up effects. It is fairly similar to a nudging technique but does not exhibit weaknesses such as frequency aliasing and signal damping. Following the analysis performed at the end of the forecast (or background) model trajectory (referred to as “FORECAST” first trajectory, with analysis time at the 4th day of the cycle), a classical forward scheme would continue straight on from this analysis, integrating from day 7 until day 14. Instead, the IAU scheme rewinds the model and starts again from the beginning of the assimilation cycle, integrating the model for 7 days (referred to as “BEST” second trajectory) with a tendency term added in the model prognostics equations for temperature, salinity, sea surface height, horizontal velocities and sea ice concentration. The tendency term (which is equal to the increment divided by the length of the cycle) is modulated by an increment distribution function. The time integral of this function equals 1 over the cycle length. In practice, the IAU scheme is more costly than the “classical” model correction (increment applied on one time step) because of the additional model integration (“BEST” trajectory) over the assimilation window. The first guess at appropriate time (FGAT) method (Huang et al., 2002) is used, which means that the forecast model equivalent of the observation for the innovation computation is taken at the time for which the data is available, even if the analysis is delayed. The concept of “pseudo-observations” or “Observed-No Change” (innovation equal to zero) has also been used to overcome the deficiencies of the background errors, in particular for extrapolated and/or poorly observed variables. We apply this approach to the barotropic height and

the 3-D coastal salinity at river mouths and all along the coasts (run off rivers). Pseudo-observations are also used for the 3-D variables T, S, U and V under the ice on the one hand, and between 6° S and 6° N below a depth of 200 m on the other hand. These observations are geographically positioned on the analysis grid points rather than on a coarser grid in order to avoid generating aliasing on the horizontal dimension. The time of these observations is the same as for the analysis, namely the fourth day of a 7-day assimilation cycle. Lastly, a Mean Dynamic Topography (MDT) derived from observations is used as a reference for SLA assimilation.

R&D activities have been conducted at Mercator Ocean these last years to improve the GLO_HR system and correct some deficiencies of the previous system PSY4V2R1 which produced CMEMS V2 GLO_HR analyses and forecasts. The ocean/sea-ice model and the assimilation scheme benefited of the following updates:

Concerning the physical model:

- The bathymetry used in the system benefited from a specific correction for Indonesian Sea inherited from the INDESO system (Tranchant et al., 2016).
- A relaxation toward the World Ocean Atlas 2013 (WOA 2013) temperature (Locarnini et al., 2013) and salinity (Zweng et al., 2013) climatology for the 2005-2012 period has been added at Gibraltar and Bab-el-Mandeb straits.
- 50% of the surface model currents are now used in the computation of the flux of momentum from the surface wind stress to the surface ocean.
- The monthly runoff climatology is built with data on coastal runoffs and 100 major rivers from the Dai et al. (2009) database (instead of Dai and Trenberth (2002) for PSY4V2R1). This database uses new data, mostly from recent years, streamflow simulated by the Community Land Model version 3 (CLM3) to fill the gaps, in all lands areas except Antarctica and Greenland. In addition, we built the runoff fluxes coming from Greenland and Antarctica ice sheets and glaciers melting using the Altiberg icebergs database project (Tournadre *et al.*, 2013). This complements the estimate of Silva et al. (2006) for Antarctica.
- As the Boussinesq approximation is applied to the model equations, conserving the ocean volume and varying its mass, the simulations do not properly directly represent the steric effect on the sea level (Greatbatch, 1994). For this reason, the global steric effect has been computed as the gradient between two successive daily global mean dynamic heights (vertical integration, from the surface to the bottom, of the specific volume anomaly). This time-evolving correction is added as a spatial constant to the sea level in the simulation. This improves the comparison between the model and the sea level observation (the latter being unfiltered from the steric component).
- Large-scale correction of precipitations (no change of synoptic patterns like cyclones and of interannual signal) has been performed using satellite data (PMWC climatology 1992-2006), except at high latitudes (poleward of 65°N and 60°S). The mean bias compared with PMWC is reduced from 0.47 to 0.19 mm/day. Nevertheless, we noticed in the first years of the simulation that the concentration/dilution water flux injected too much salt in the model, probably due to an excessive evaporation in summer at mid-latitudes. The salt penetrates deeper during winter by subduction and mixes. To avoid this slow salinity drift, a constant of 2.3 10^{-6} kg/m^2/s (0.2 mm/day) has been removed to the concentration/dilution water flux term.
- In order to avoid any mean sea-surface-height drift due to the large uncertainties in the water budget closure, the following treatments were applied:

- A trend of 2.2 mm/year has been added to the runoffs in order to somehow represent the recent estimate of the global mass addition to the ocean (from glaciers, land water storage changes, Greenland and Antarctica ice sheets mass loss) (Chambers et al., 2016).
- The surface freshwater budget is set to zero at each time step with a superimposed seasonal cycle (Chen et al., 2005).

Concerning the assimilation:

- CMEMS sea ice concentration "SEAICE_GLO_SEAICE_L4_NRT_OBSERVATIONS_011_001 (OSI-401)" is now assimilated in the system in a monovariate/monodata mode.
- CMEMS OSTIA SST "SST_GLO_SST_L4_NRT_OBSERVATIONS_010_001" is now assimilated in the new system, instead of AVHRR SST. A particular attention has been devoted to the computation of the model equivalent.
- In addition to the quality control based on temperature and salinity innovation statistics (detection of spikes, large biases, …), already present in the previous system, a second quality control has been developed and is based on dynamic height innovation statistics (detection of small vertically constant biases).
- A new MDT, based on the "CNES-CLS13" MDT (Rio et al., 2014) with adjustments made using high resolution analysis and with an improved Post Glacial Rebound (also called Glacial Isostatic Adjustment), has been used. This new product also takes into account the last version of the GOCE geoid and is replacing the MDT named "CNES-CLS09" derived from observations (Rio et al., 2011) which was used in the previous system.
- A consistent SLA dataset ("SEALEVEL_GLO_SLA_L3_REP_OBSERVATIONS_008_018", with a 20-year altimeter reference period) is assimilated all along the hindcast calibration run.
- The CORA 4.1 CMEMS in situ database "INSITU_GLO_TS_REP_OBSERVATIONS_013_001_b" has been assimilated for the hindcast calibration run of the system (2007-2015). This database includes temperature and salinity vertical profiles from the sea mammal (elephant seals) database (Roquet et al., 2011) to compensate for the lack of such data at high latitudes.
- In order to refine the prescription of observation errors, adaptive tuning of observation errors for the SLA and SST (Desroziers et al., 2005) has been implemented. The method consists in the computation of a ratio which is a function of observation errors, innovations and residuals. It helps correcting inconsistencies on the specified observation errors. As a first guess of the method, the initial error matches the one used in the previous system where the observation error variance was increased for the assimilation of SLA near the coast and on the shelves, and for the assimilation of SST near the coast (within 50 km of the coast).
- New 3D observation errors files for the assimilation of in situ temperature and salinity data have been re-computed from the GLORYS2V2 Mercator reanalysis.
- A week constraint towards the WOA 2013 (2005-2012) climatology on temperature and salinity in the deep ocean (below 2000 m) has been included in the two assimilation schemes to prevent drifts in temperature and salinity and as a consequence to obtain a better representation of the sea level trend at global scale in the system. The method consists in assimilating vertical climatological profiles of temperature and salinity at large scale and below 2000 m, using a non-Gaussian error at depth. This allows the system to capture a potential climate drift at depth.
- The time window for the 3D-Var bias correction moved from 3 to 1 month.
- In the previous system, the SSH increment was the sum of barotropic and dynamic height increments. Dynamic height increment was calculated from the temperature and salinity increments. In the current system, we directly use the SSH increment given by the analysis to take into account, among other things, the wind effect.

- The uncertainties in the MDT estimate and the sparsity of the observation networks (both altimetry and in situ profiles) on the 7-day assimilation window do not allow to accurately estimate the observed global mean sea level. Therefore, the global mean increment of the total sea surface height is set to zero.
- The matrices of covariance of errors needed for data assimilation are defined using anomalies of the different variables coming from a simulation in which a 3D-Var large scale bias correction of T, S has been performed (instead of using a free run –with no data assimilation- as was done in the previous version of the system). Moreover, these anomalies are spatially filtered in order to retain only the effective model resolution and in order to avoid injecting noise in the increments.
- The velocity increments are no more cut off in the equatorial band, as was the case in the previous system between 6°S and 6°N.

A simulation for the calibration of the PSY4V3R1 system was run over the October 2006 - June 2016 period, starting from 3D temperature and salinity initial conditions based on the EN4 climatology. The PSY4V3R1 system starts operation in October 2016. Note that two other simulations over the same period are available. The first one is a free simulation (without any data assimilation) and the second one only benefits from the 3D-Var large-scale biases correction in temperature and salinity.

System name	Domain	Resolution	Model version	Assimilation software version	Assimilated observations	Status of production
HR global	global	1/12° on the horizontal + 50 levels on the vertical	ORCA12 + LIM2 EVP + NEMO 3.1 + 3-hourly atmospheric forcing from ECMWF + Bulk CORE + 50% of model surface currents used for surface momentum fluxes + updated runoff from Dai et al., 2009 + runoff fluxes coming from Greenland and Antarctica + Addition of a trend (2.2mm/year) to the runoff	SAM2 (SEEK Kernel) + IAU + 3D-Var bias correction (1 month time window) + Addition of a second QC on T/S vertical profiles + Adaptive tuning of observation errors for SLA and SST + New 3D observation errors files for assimilation of in	CMEMS OSTIA SST + CMEMS Sea Ice Concentration + CMEMS SLA + in situ profile from CMEMS database + MDT adjusted based on CNES-CLS13 + WOA 2013 climatology (temperature and salinity) below 2000 m (assimilation using a non-Gaussian error at depth)	Weekly 7-day hindcast, and nowcast + Daily 10-day forecast (update of atmospheric forcing)

			+ Global steric effect added to the sea level + Addition of seasonal cycle for surface mass budget + Correction of precipitations using satellite data + Correction of the concentration/dilution water flux term + Relaxation toward WOA 2013 at Gibraltar and Bab-el-Mandeb	situ profiles + Use of the SSH increment instead of the sum of barotropic and dynamic height increments + Global mean increment of the total SSH is set to zero		

Table 6: Synthetic description of GLO_HR production system

III VALIDATION FRAMEWORK

Most of the scientific assessment framework for the GLO_HR global system is documented in Lellouche et al. (2013) and is summarized in the table of Metrics (Table 7). In this document we will emphasize accuracy metrics (data assimilation scores and CLASS 4 metrics) when available. Results will be presented in the following sections for each type of product (region, variable).

variable	Region	Type of metric	MERSEA/GODAE classification	Reference observational dataset
3D temperature	Global, and regional basins	Residual Error=obs-model Time evolution of RMS error on 0-500m Vertical profile of mean error.	CLASS4	CMEMS: CORIOLIS T (z) profiles
3D salinity	Global, and regional basins	Residual Error=obs-model Time evolution of RMS error on 0-500m Vertical profile of mean error.	CLASS4	CMEMS: CORIOLIS S(z) profiles
Sea level anomaly (SLA)	Global, and regional basins	Residual Error=obs-model Time evolution of RMS and mean residual error	Data assimilation statistics	CMEMS: On track AVISO sla observations from Jason3, Saral Altika and Cryosat
Sea surface height	At tide gauges (Global but near coastal regions)	Residual Error=model-obs Time series correlation and RMS error	CLASS4	Tide gauges sea level time series from GLOSS, BODC, Imedea, WOCE, OPPE and SONEL
Sea Surface Temperature SST	Global, and regional basins	Residual Error=obs-model Time evolution of RMS and mean error	Data assimilation statistics	CMEMS: OSTIA SST
Surface layer zonal current U	Global, and regional basins	Residual error=obs-model Mean error and vector correlation	CLASS4	CMEMS: SVP drifting buoys
Surface layer meridional current V	Global, and regional basins	Residual Error=obs-model Mean error and vector correlation	CLASS4	CMEMS: SVP drifting buoys

Sea ice concentration	Antarctic and Arctic regions	Visual inspection of seasonal and interannual signal	CLASS1	CMEMS: OSI TAC Sea ice concentration
Sea ice concentration	Antarctic and Arctic regions	Residual Error=obs-model Time evolution of RMS and mean error	data assimilation statistics	CMEMS: OSI TAC Sea ice concentration
Sea ice concentration	Antarctic and Arctic regions	Time evolution of sea ice extent	CLASS3	NSIDC sea ice extent from SSM/I observations
Monthly 3D T and S	Global	Visual inspection of seasonal and interannual signal	CLASS1	Levitus 2013 monthly climatology of temperature and salinity
T, S, U, V, SSH, atmospheric forcings	Global, at CLASS2 locations	Visual inspection of high frequencies, comparisons with observed time series	CLASS2	CMEMS: CORIOLIS
SLA and SST	Tropical basins	Visual inspection of hovmueller diagrams and comparisons with satellite observations	CLASS1	CMEMS SL and OSI TACs
3D U and V	Global	Visual inspection of volume transports through sections	CLASS3	litterature

Table 7: List of metrics that were computed to assess the GLO_HR products.

VALIDATION RESULTS

This document synthesizes the results of the scientific qualification of the GLO HR monitoring and forecasting system. The reference period for this scientific qualification exercise is the **year 2015**. Some diagnostics computed over the whole hindcast run (2007-2016) are also shown. In the next sections of the document, we present hindcast statistics by region and depth layers. As the system started running operationally in September 2016, and due to computer resource restrictions, no forecast is available before this date. In consequence, even if the performance of the forecast has been checked with the data assimilation system, and no degradation is measured with respect to the V2 system, the forecast **statistics at several forecast length that really quantify the improvements of the system will only be added to this report at the end of 2016.**

Estimated Accuracy Numbers (EAN) for GLO_HR analyses were computed in 11 regions corresponding to the main basins of the global ocean: NAT, TAT, MED, SAT, IND, SPA, TPA, NPA, ARC, ACC, GLO (see Figure 31 in appendix). The modeled physical variables were compared to assimilated observations, and to independent observations when available. When possible, the V2.3 and V2 global ocean estimates and EANs were intercompared to ensure the consistency of the results, and quantify the improvements between V2 and V2.3 (verification of non regression).

III.1 Global Ocean: GLO

III.1.1 Temperature

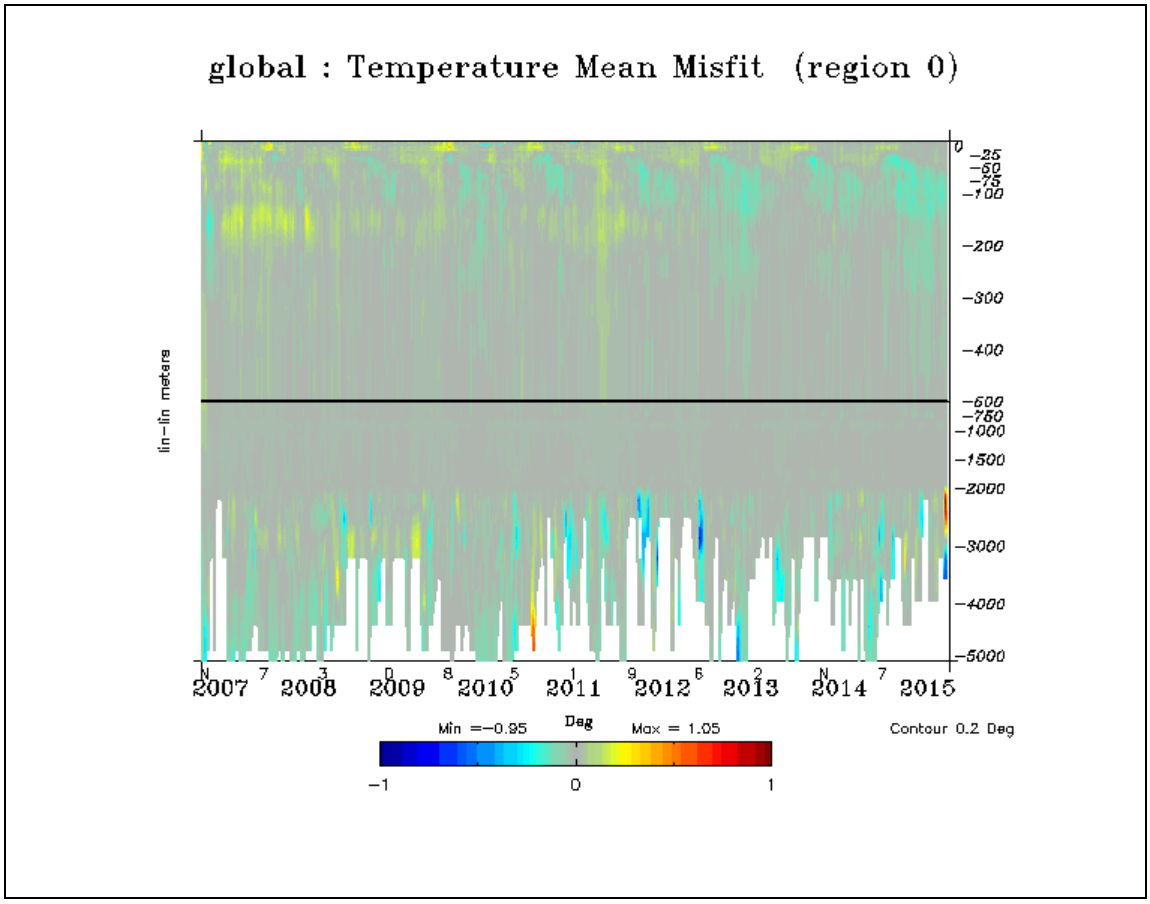

Figure 1: Average temperature misfit in K (observation – forecast) from data assimilation statistics over time and depth for the whole hindcast run (2007-2015).

The V2.3 GLO HR system experiences a slight warm bias (negative observation – forecast difference) in subsurface (25-500m) on global average as shown by Figure 1. This bias seems stronger during the last years 2013-2015. The average bias maps of 2015 (Figure 2) show that as in V2 (not shown) part of this signal comes from the strong interannual ENSO signals in the Tropical Pacific where the near surface bias is also warm, as well as in the ACC and Gulfstream. Seasonal cold surface biases appear in the mid latitudes, linked with a lack of stratification during summer. Summer warming is injected too deep and results in subsurface spurious warming and too shallow mixed layer. Although these biases stay small (compensate) on global average, the temperature biases are slightly stronger in the V2.3 system than in the V2 system, which explains also higher RMS errors on average in the V2.3 system (Table 1).

a) TEMP mean OBS-MODEL 0-5 m 2015

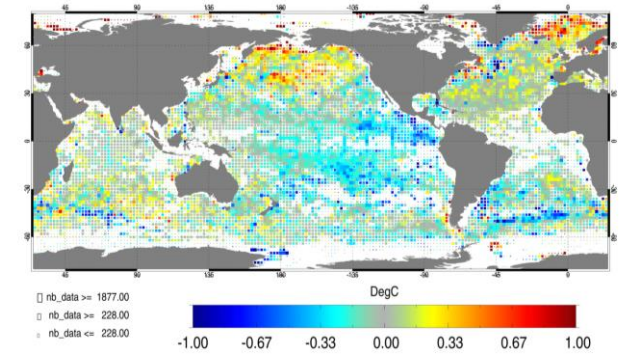

b) TEMP RMS OBS-MODEL 0-5 m 2015

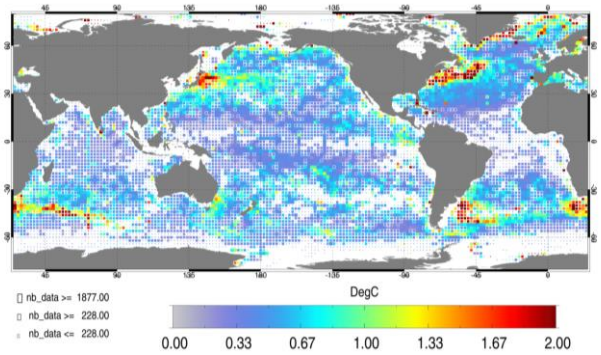

c) TEMP mean OBS-MODEL 5-100 m 2015

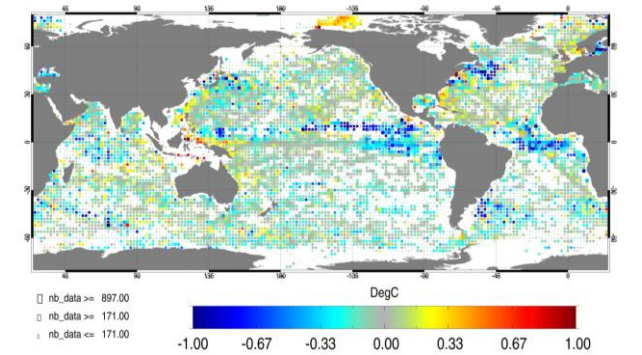

d) TEMP RMS OBS-MODEL 5-100 m 2015

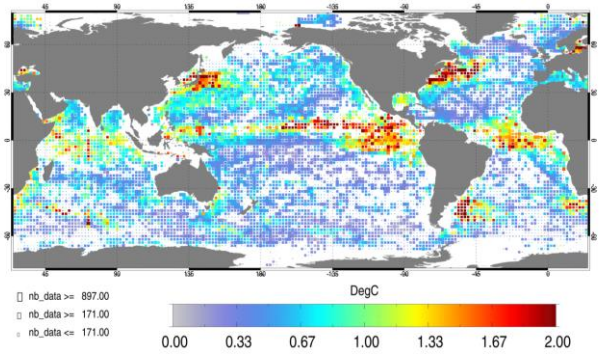

e) TEMP mean OBS-MODEL 100-300 m 2015

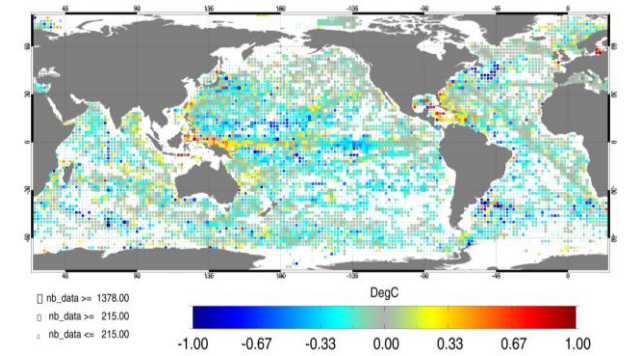

f) TEMP RMS OBS-MODEL 100-300 m 2015

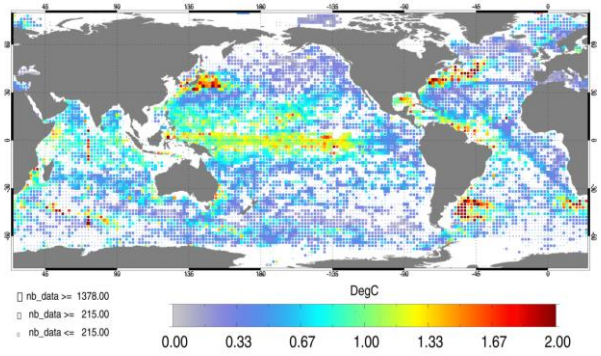

Figure 2: mean (a,c, and e) and RMS (b,d, and f) *observation-analysis* temperature (K) differences over the calibration year 2015, averaged in the 0-5 m (a and b) 5-100m (c and d) and 100-300m (e and f) layers. Differences are computed at the observations' time and location. For each pixel statistics are computed in 2°x2° bins, and the size of the pixel is proportional to the number of observations falling into the bin.

3D T (K)	Hindcast		Forecast day 3	
	Mean misfit	RMS misfit	Mean misfit	RMS misfit

	V2	V2.3	V2	V2.3	V2	V2.3	V2	V2.3
0-5m	-0.02	-0.03	0.57	0.65	tbc	tbc	tbc	tbc
5-100m	-0.01	-0.05	0.86	0.89	tbc	tbc	tbc	tbc
100-300m	-0.05	-0.06	0.73	0.78	tbc	tbc	tbc	tbc
300-800m	-0.02	-0.03	0.41	0.43	tbc	tbc	tbc	tbc
800-2000m	0.00	0.00	0.15	0.17	tbc	tbc	tbc	tbc
2000-5000m	-0.03	0.02	0.14	0.22	tbc	tbc	tbc	tbc
0-5000m	-0.01	-0.01	0.38	0.41	tbc	tbc	tbc	tbc

Table 8: GLO RMS and average temperature misfits in K (observation-model) with respect to the CORIOLIS in situ observations, in contiguous layers from 0 to 5000m, for the calibration year 2015.

III.1.2 Salinity

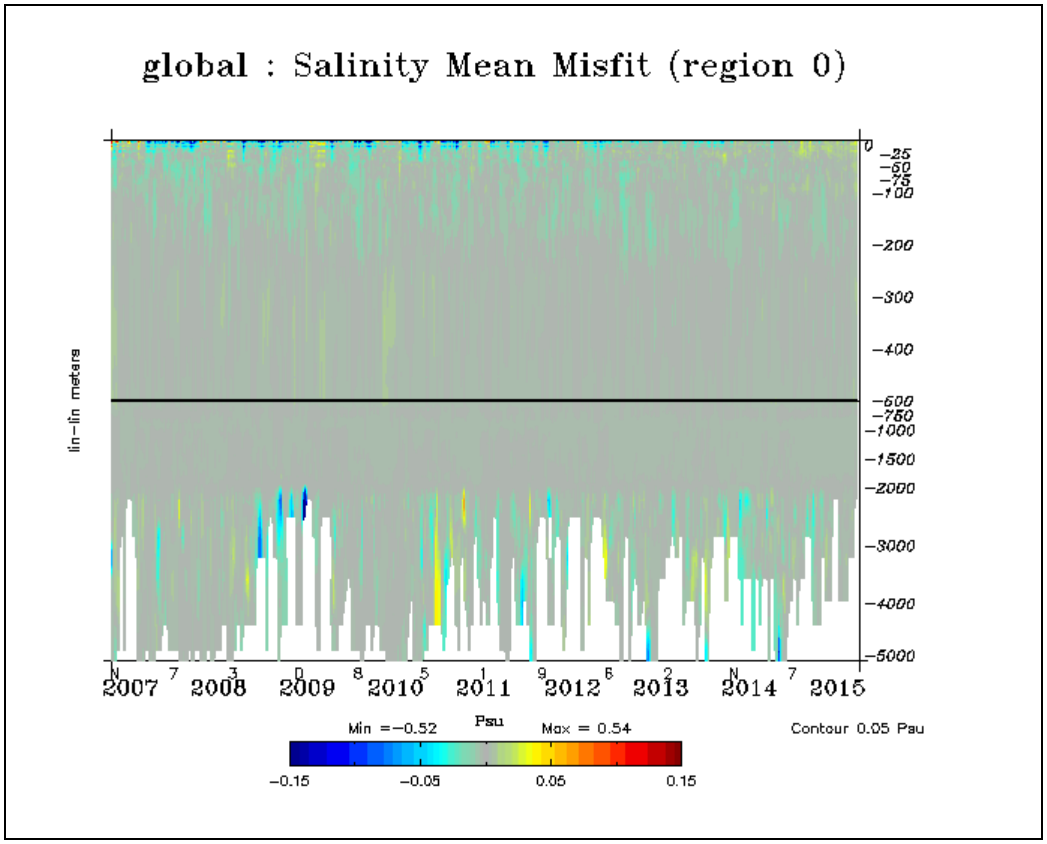

Figure 3: Average salinity misfit in psu (observation – forecast) from data assimilation statistics over time and depth, for the whole hindcast run (2007-2015).

a) SAL mean OBS-MODEL 0-5 m 2015	b) SAL RMS OBS-MODEL 0-5 m 2015

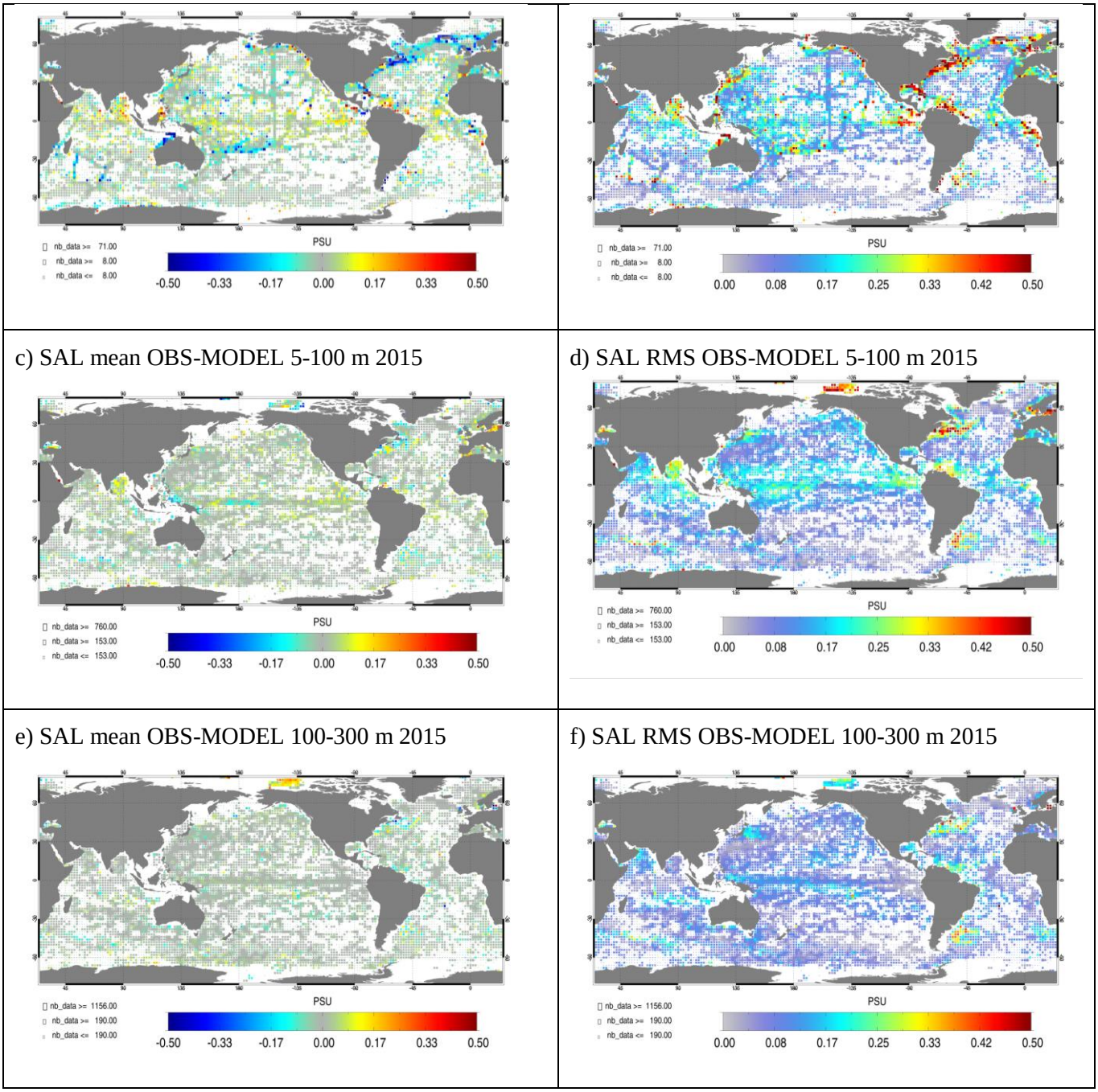

Figure 4: mean (a, c, and e) and RMS (b, d, and f) *observation-analysis* salinity (psu) residual differences over the calibration year 2015, averaged in the 0-5 m (a and b) 5-100m (c and d) and 100-300m (e and f) layers. Differences are computed at the observations' time and location. For each pixel statistics are computed in 2°x2° bins, and the size of the pixel is proportional to the number of observations falling into the bin.

As can be seen in Figure 3 and Figure 4 the salinity biases are very small in the V2.3, and salinity errors (mean and RMS) have been reduced from V2 to V2.3 as shown by Table 9 . A strong surface bias (GLO HR is too salty) is observed in the North Atlantic in 2015. A fresh bias due to excess precipitations is still present in V2.3 in the tropical band (Figure 4a) but has been strongly reduced with respect to V2

(not shown). In subsurface, near 100m depth, the RMS errors in the Tropical Pacific may be increased in 2015 due to the El Nino event. Fresh biases are observed in the Arctic in the 100-300m layer.

3DS(PSU)	Hindcast				Forecast day 3			
	Mean misfit		RMS misfit		Mean misfit		RMS misfit	
	V2	V2.3	V2	V2.3	V2	V2.3	V2	V2.3
0-5m	0.019	0.005	0.266	0.199	tbc	tbc	tbc	tbc
5-100m	0.000	0.005	0.207	0.166	tbc	tbc	tbc	tbc
100-300m	-0.006	-0.002	0.118	0.107	tbc	tbc	tbc	tbc
300-800m	0.000	0.000	0.055	0.057	tbc	tbc	tbc	tbc
800-2000m	0.001	0.001	0.024	0.026	tbc	tbc	tbc	tbc
2000-5000m	-0.001	-0.003	0.013	0.017	tbc	tbc	tbc	tbc
0-5000m	0.000	0.000	0.068	0.061	tbc	tbc	tbc	tbc

Table 9: GLO RMS and average salinity misfits in psu (observation-model) with respect to the CORIOLIS in situ observations, in contiguous layers from 0 to 5000m, for the calibration year 2015.

III.1.3 SST

OSTIA products are now assimilated in the GLO_HR system, as can be seen in the RMS errors of Figure 6. Some large scale biases with respect to OSTIA are reduced in V2.3 with respect to V2 (cold biases in the Indian, Eastern South Pacific, and western North Pacific). On the other hand, warm biases get stronger in V2.3, especially in regions of strong interannual warm signals such as the Eastern Tropical Pacific where El Nino took place in 2015, but also in the ACC, the Gulf Stream and the Greenland Current, resulting in a warm bias in global average of around 0.1 K, as shown in Table 1. The surface error patterns are consistent with the near surface temperature biases of Figure 2. The cold near surface bias in the mid latitudes is not diagnosed in SST, suggesting that OSTIA might be colder than in situ observations in these regions. Figure 6 suggests that OSTIA, as NOAA AVHRR, are colder than the in situ near surface observations on global average, especially at the end of the period. Figure 6 also shows seasonal fluctuations of the SST biases on global average as the lack of stratification in the model causes stronger mid latitude cold biases during (boreal) summer. The drop in the number of in situ surface data at the end of the period is due to the use of NRT observations, where most of the surface observations do not have sufficient quality flag.

NB: Regional EAN for SST could not be computed here and will be added to the next version of this document.

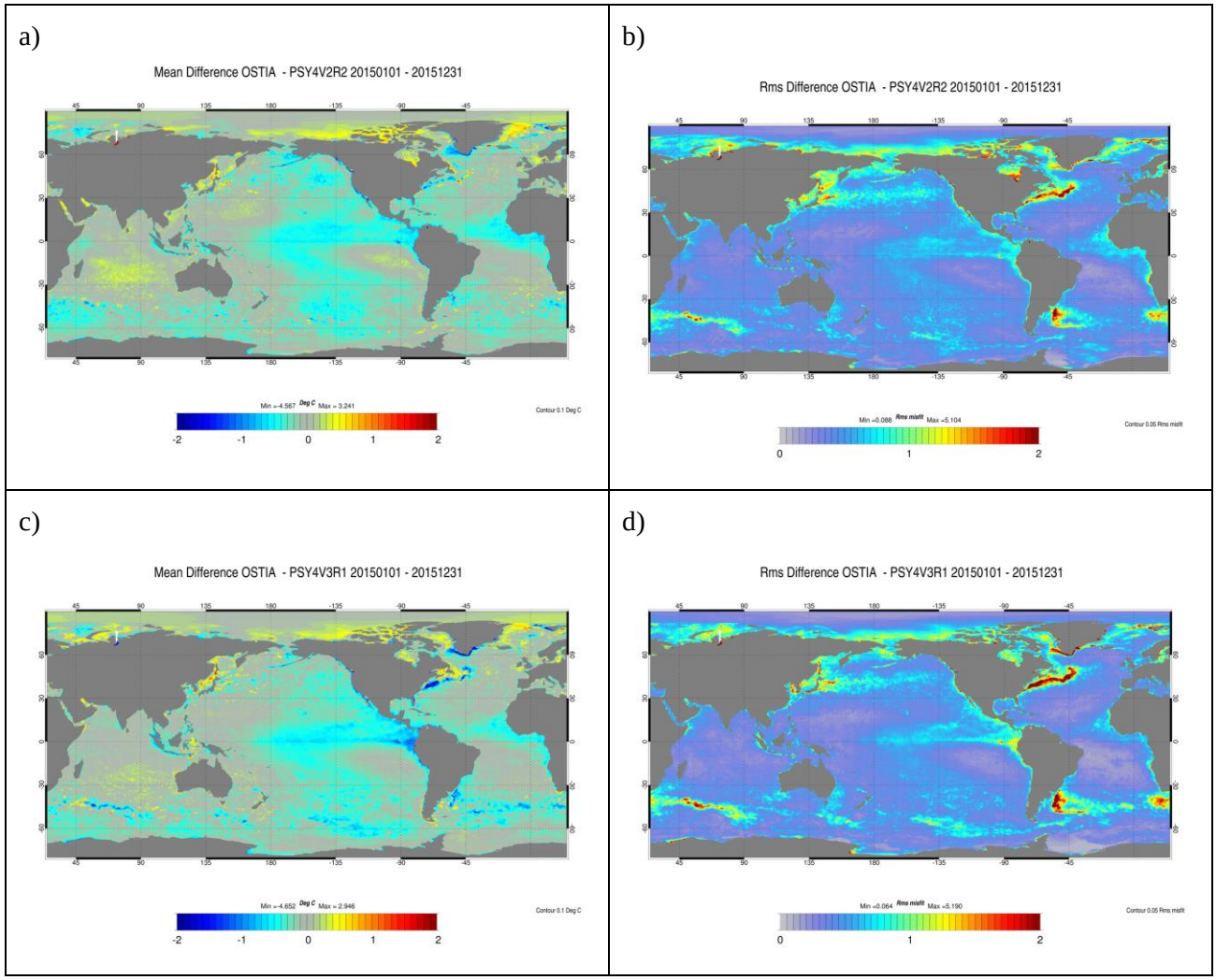

Figure 5: Mean (a and c) and RMS (b and d) residual SST errors (K) OSTIA – GLO_HR V2 (a and b) and OSTIA – GLO_HR V2.3 (c and d), computed for the calibration year 2015.

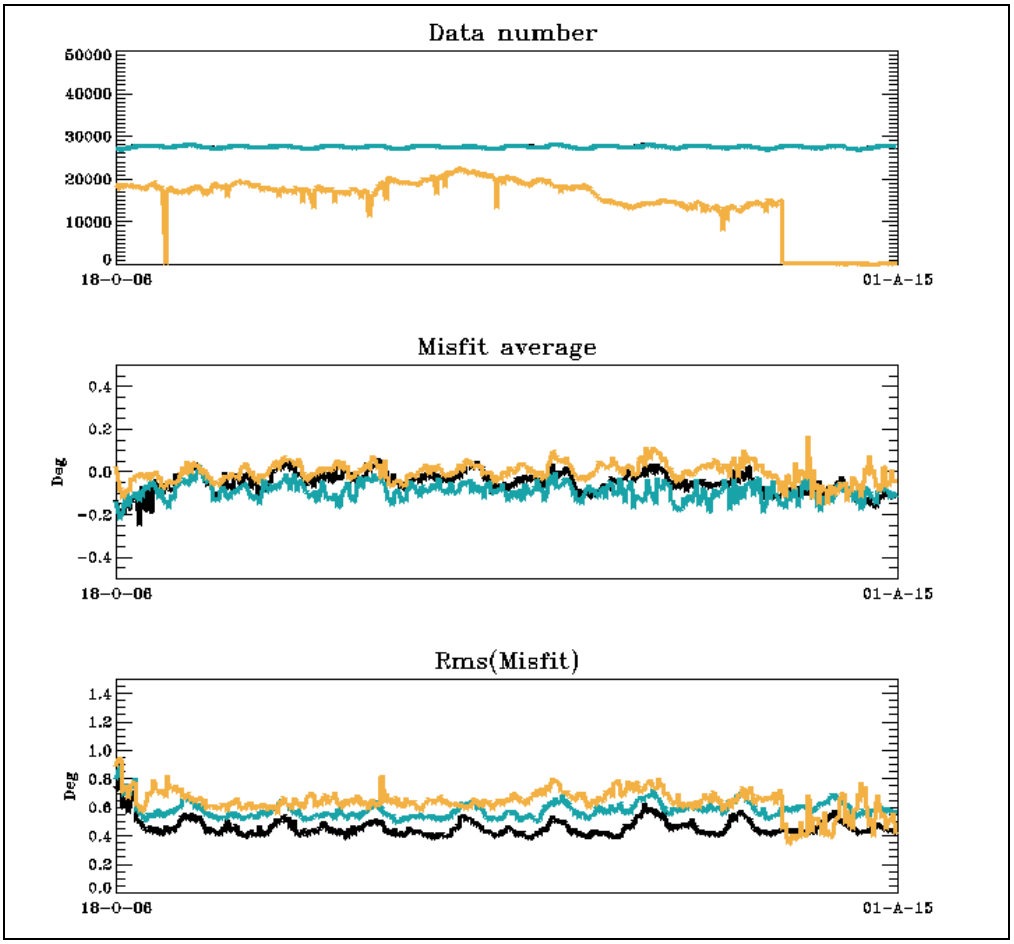

Figure 6 : The number of OSTIA (black line, assimilated data), NOAA AVHRR (blue line, independent data) and in-situ (orange line, independent data) SST observations is shown in the top panel. SST (°C) global misfits average (middle) and rms (bottom) for assimilated OSTIA SST observations (black line) and NOAA AVHRR observations (blue line), and in situ observations (orange line), for the whole hindcast run (October 2006- august 2015).

SST (K)	Hindcast				Forecast			
	Mean misfit		RMS misfit		Mean misfit		RMS misfit	
	V2	V2	V2	V2.3	V2	V2.3	V2	V2.3
GLO	-0.01	-0.1	0.5	0.45	tbc	tbc	Tbc	tbc

Table 10: GLO RMS and average SST misfits in K (observation-model) with respect to assimilated observations (NOAA AVHRR for V2, and OSTIA for V2.3).

III.1.4 SLA

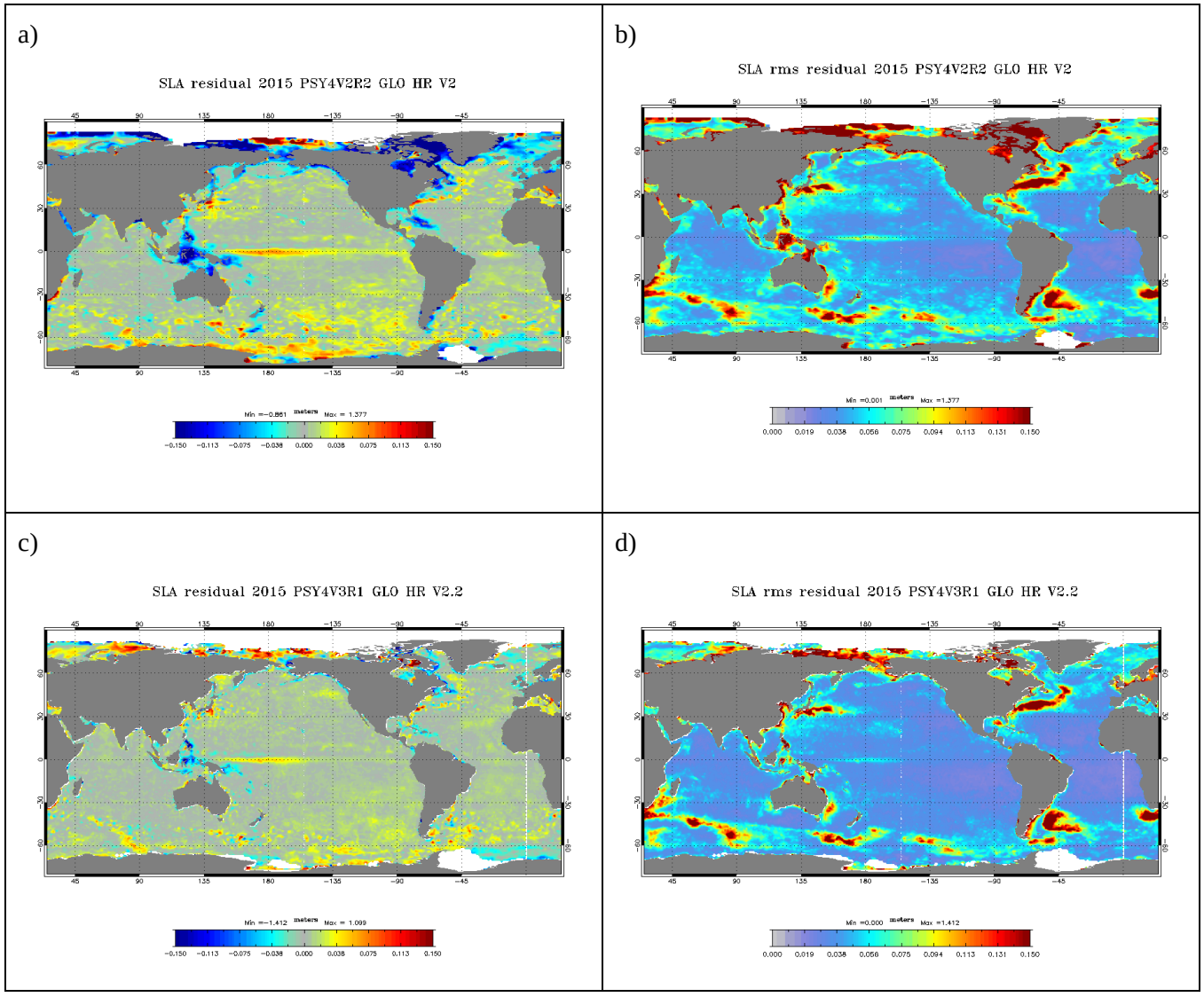

Figure 7: Mean residual (observation – analysis) error of SLA (m) in GLO_HR V2 (a) and V2.3 (c), and RMS residual error of SLA (m) in GLO_HR V2 (b) and V2.3 (d)

As shown in Figure 7, the SLA mean and RMS errors have been considerably reduced in the V2.3 system with respect to the previous V2 system, in nearly all regions of the ocean. This is mainly due to the use of the Desroziers criterion to adapt the observations errors online, which yield to more information from the observations being used, especially in the near coastal regions (not shown). However, some patches of RMS errors increases can be detected in the ACC, Zapiola eddy and inside the Gulf Stream and Agulhas currents (Figure 8).

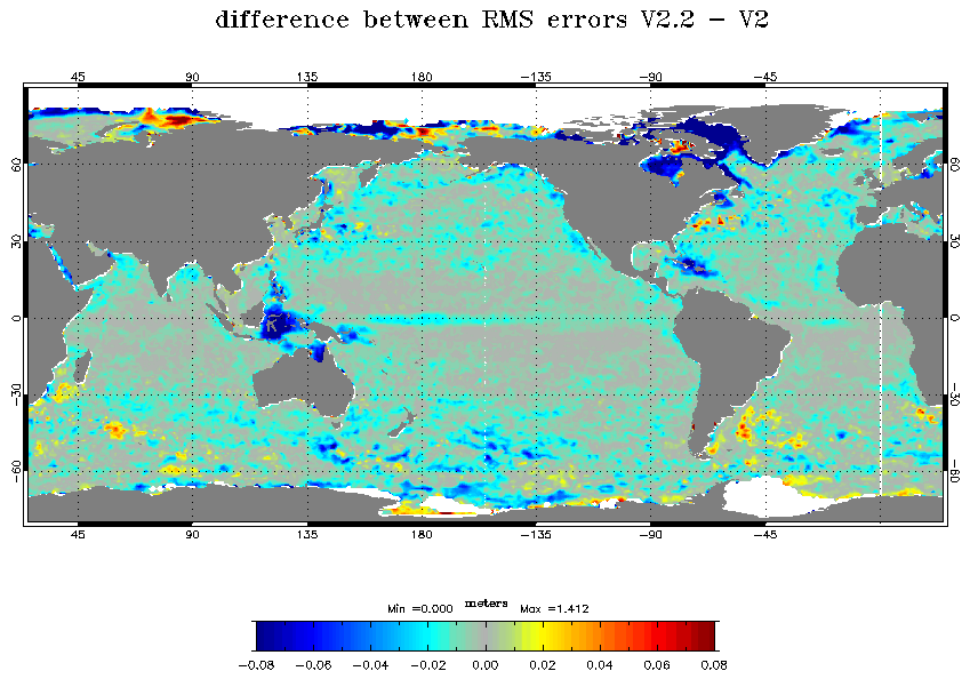

Figure 8: Difference between RMS residual (observation – analysis) errors of SLA (m) in GLO_HR V2.3 and V2. Negative values indicate that the RMS of residual errors of SLA are weaker in GLO_HR V2.3. than in v2.

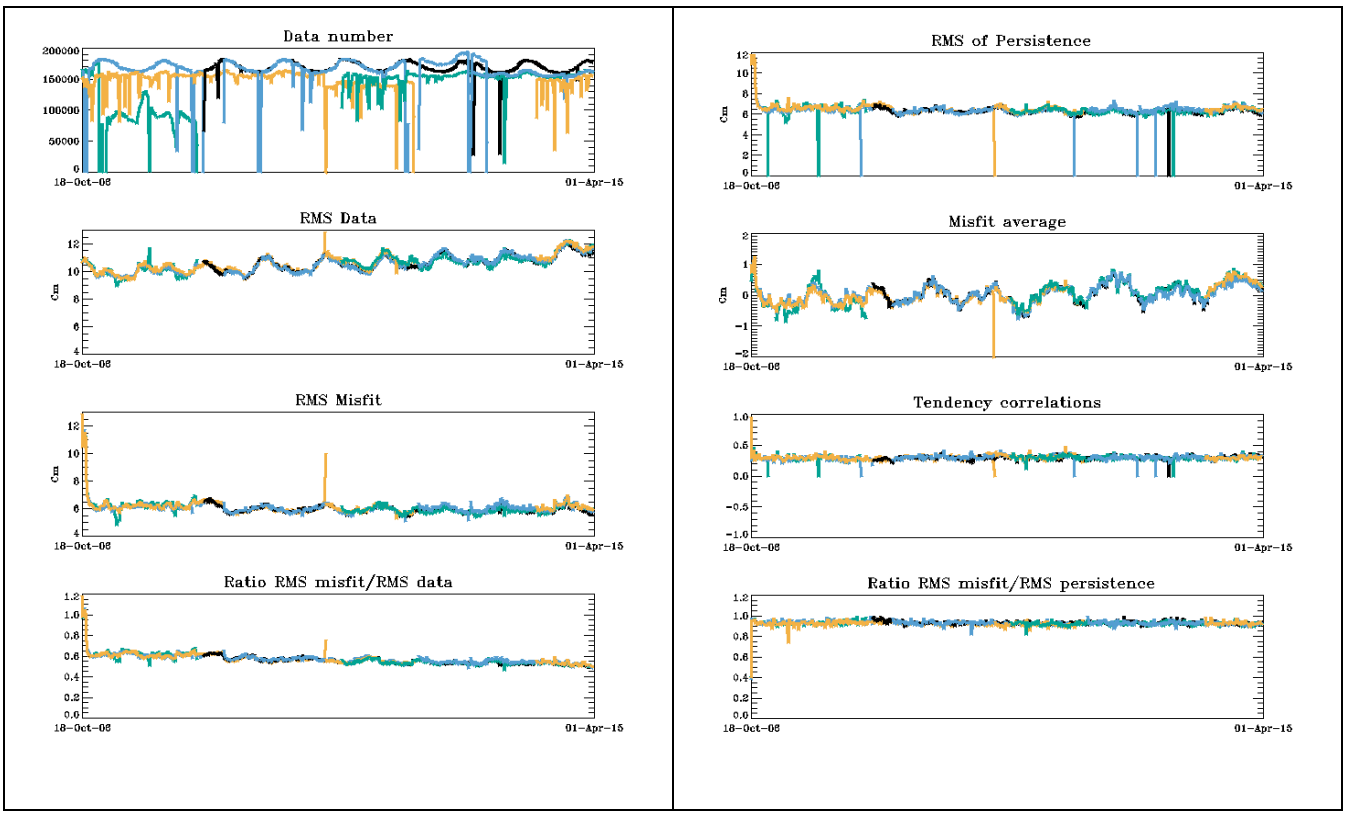

Figure 9: SLA (cm) data assimilation statistics for the HR global system with respect to along track observations (green: geosat2 and then cryosat2, blue: jason1, jason1 new orbit, Jason1 geodetic and then Altika, orange: envisat, Envisat new orbit, and then HY2, black: jason2), for the whole hindcast run (2007-2015).

The stability over time of the accuracy in terms of SLA is illustrated in Figure 9 . The RMS error is 6 cm on average over the 2007-2015 period and the average misfit oscillates between positive and negative values resulting in a small 0.63 cm bias in Table 11. The SLA bias is 0.3 cm higher in V2.3 than in V2, but the RMS misfit has improved from 6.3 cm to 5.5 cmV2.3, suggesting that the SSH variability is closer to SLA observations in V2.3 than in V2.

Seal Level Anomaly (cm)	Hindcast				Forecast day 3			
	Mean misfit		RMS of misfit		Mean misfit		RMS misfit	
	V2	V2.3	V2	V2.3	V2	V2.3	V2	V2.3
GLO	0.35	0.63	6.30	5.50	tbc	tbc	Tbc	tbc

Table 11: GLO RMS and average SLA misfits in cm (observation-model) with respect to altimetric observations.

III.1.5 Sea Ice

Sea ice concentrations from OSI TAC are assimilated in GLO_HR V2.3, which was not the case in V2 where no sea ice concentration data assimilation was performed. This data assimilation consistently reduces the mean and RMS errors of GLO_HR V2.3 in Sea Ice Concentrations with respect to V2, as illustrated by Figure 10.

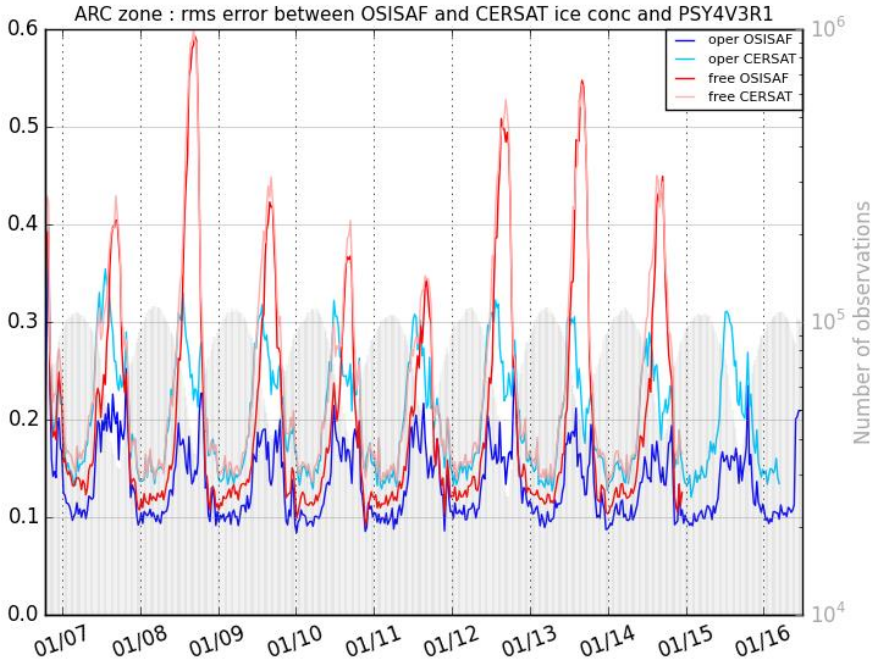

Figure 10: (observation-forecast) RMS differences of Sea ice Concentration (SIC, 0 means no ice, 1 means 100% ice cover) in the Arctic. Dark blue is the RMS error of GLO_HR with respect to assimilated OSI TAC's SIC, light blue is the RMS of GLO_HR with respect to CERSAT SIC independent observations. Dark red is the RMS error of GLO_HR twin experiment with no sea ice concentration data assimilation (free run, as in GLO HR V2) with respect to OSI TAC's observations, and light red is the same but with respect to CERSAT sea ice concentrations. The number of OSI TAC's SIC data is shown in grey (units on the right y-axis).

As shown by Figure 11, the GLO_HR system sees slightly too much ice during the beginning of the melting season in summer (up to 3% overestimation on average in both Arctic and Antarctic basins), while the mean error is stronger on average during winter (10 to 20% underestimation, depending on the year).

a)	b)

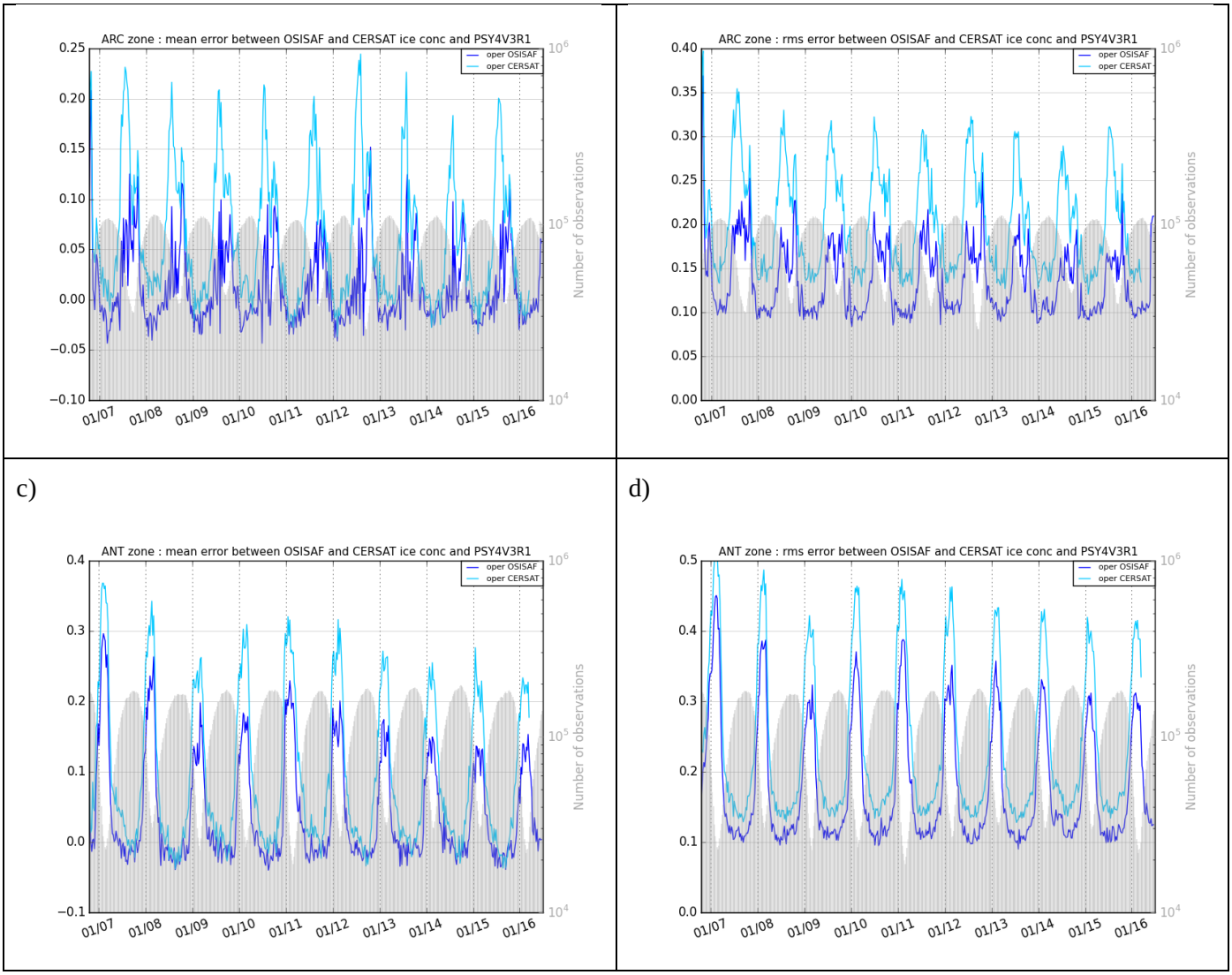

Figure 11: (observation-forecast) mean (a and c) and RMS (b and d) differences of Sea ice Concentration SIC (0 means no ice, 1 means 100% ice cover) in the Arctic Ocean (a and b) and Antarctic Ocean (c and d). Dark blue is the mean or RMS error of GLO_HR with respect to assimilated OSI TAC's SIC, light blue is the mean or RMS of GLO_HR with respect to CERSAT SIC Observations.

Sea Ice Cover (%)	Hindcast				Forecast day 3			
	Mean misfit		RMS of misfit		Mean misfit		RMS misfit	
	V2	V2.3	V2	V2.3	V2	V2.3	V2	V2.3
ARC	-20%	10%	30%	20%	tbc	tbc	Tbc	tbc
ACC	-30%	5%	40%	25%	tbc	tbc	Tbc	tbc

Table 12: GLO_HR V2.3 RMS and average Sea Ice Concentration (observation-model) with respect to OSI TAC observations.

RMS errors are also larger during the melt season in summer (up to 20% in the Arctic and 30% in the Antarctic with respect to OSI TAC's observations), and drop to less than 10% in winter. These RMS errors quantify the capacity of the system to capture weekly time changes in the ice cover.

In the Arctic, the error peaks without data assimilation happen at the sea ice cover minimum in September, while with data assimilation it is now during summer (July-August), while the Sea Ice is melting. This may be linked to the fact that the weekly assimilation of sea ice concentration is not fitted to constrain rapid changes in the sea ice cover in the marginal seas.

III.1.6 Surface currents

Near surface currents (near 15m depth) can be compared with velocities deduced from drifters (CMEMS) and ARGO floats (YoMaHa) trajectories (see Lellouche et al, 2013). We use these Eulerian comparisons to give an estimate of the surface currents errors, and quantify the improvement between V2 and V2.3.

The velocities have been slightly improved from V2 and V2.3 in terms of velocity values (2 and 3) as well as in terms of current directions (angle between observed and modelled velocities) (Figure 14).

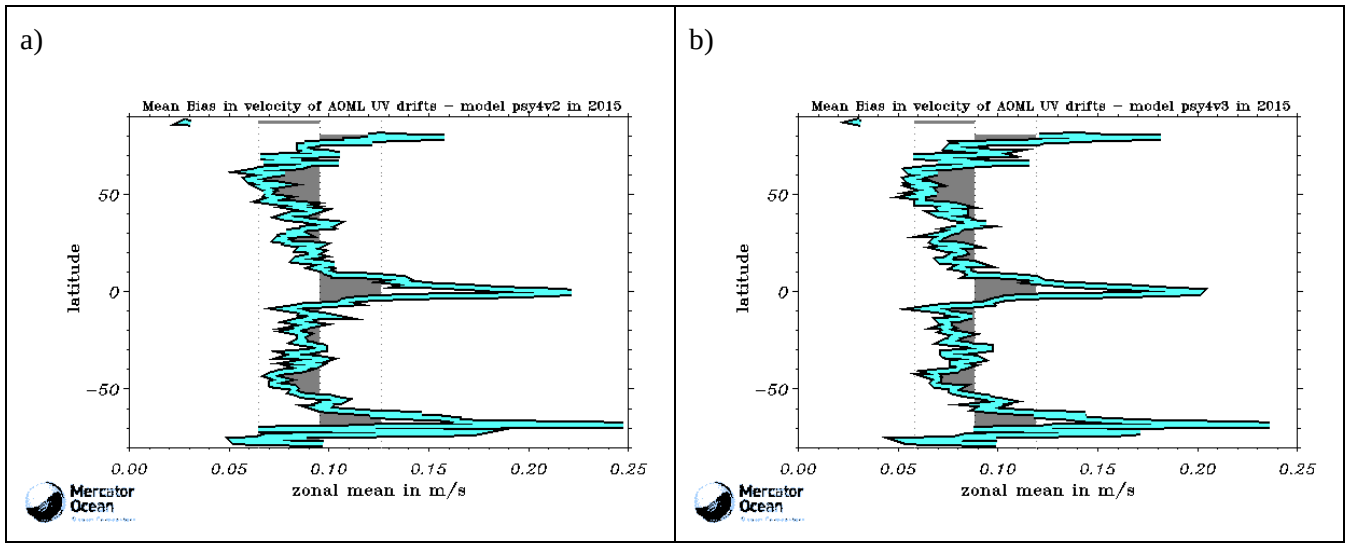

Figure 12: zonal average velocity biases (m/s) in the GLO_HR V2 (a) and GLO_HR V2.3 (b) with respect to drifters' velocities and ARGO floats velocities, over the calibration year 2015.

The location of the main currents is very well represented, as well as their variability, but large biases persist in the western tropical Pacific (very strong in 2015 because of the El Nino event) as can be seen in Figure 15, with a spurious extension of the northern branch of the South Equatorial Current. The currents magnitude is usually underestimated at mid-latitudes and overestimated in the tropics. Relative errors range from 20% to 100% locally (not shown).

EAN from these metrics will be produced for CMEMS V3.

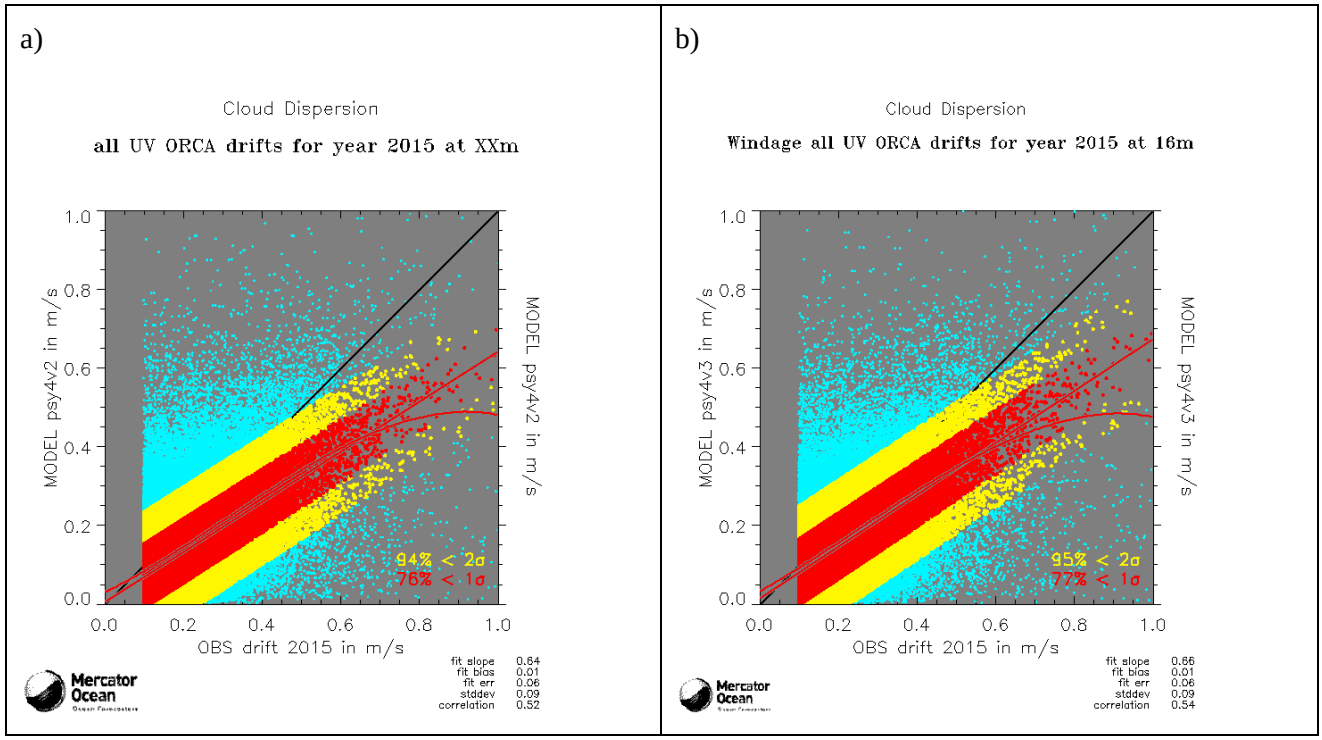

Figure 13: scatter diagrams for GLO_HR V2 (a) and GLO_HR V2.3 (b) velocities near 15 m depth with respect to drifters' velocities and ARGO floats velocities, for the calibration year 2015.

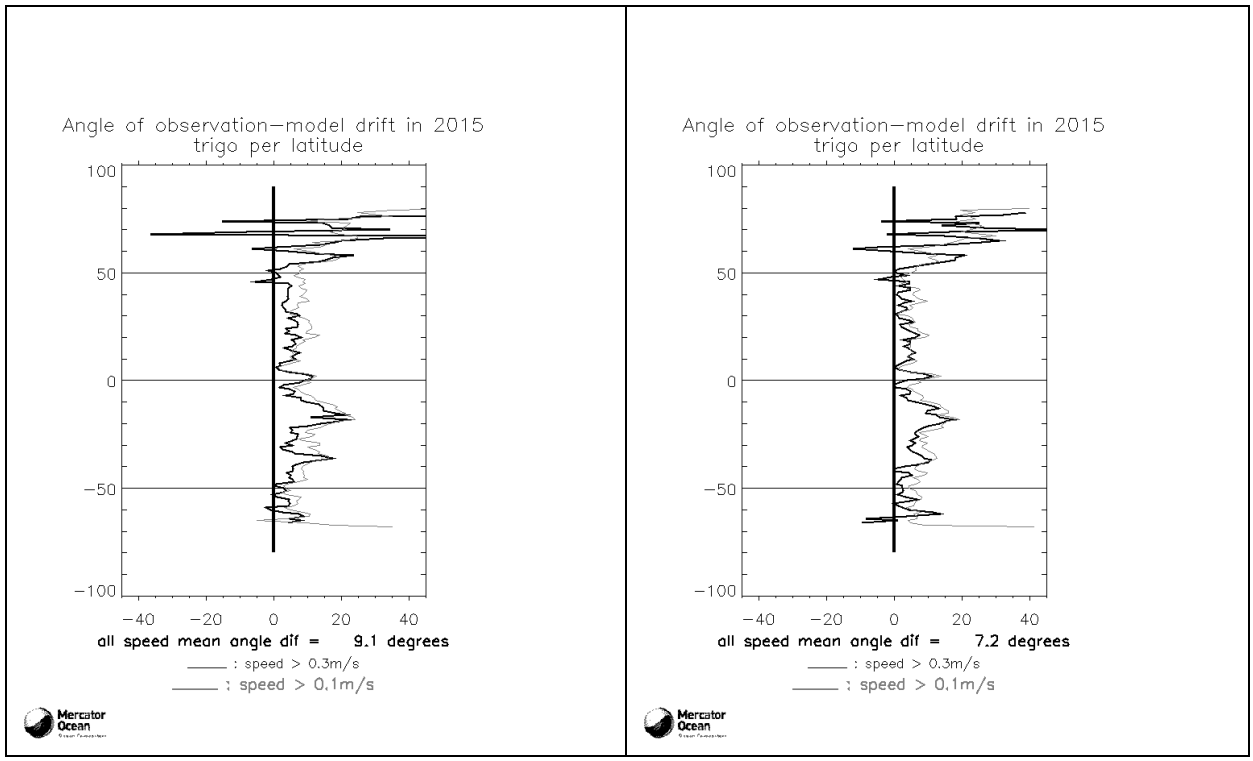

Figure 14: zonal average trigonometric angle (°) between the GLO_HR V2 (a) and GLO_HR V2.3 (b) velocity vectors and the drifters' velocities and ARGO floats velocities, over the calibration year

2015. Current velocities higher than 0.1 m/s are shown in grey and velocities higher than 0.3 m/s in black.

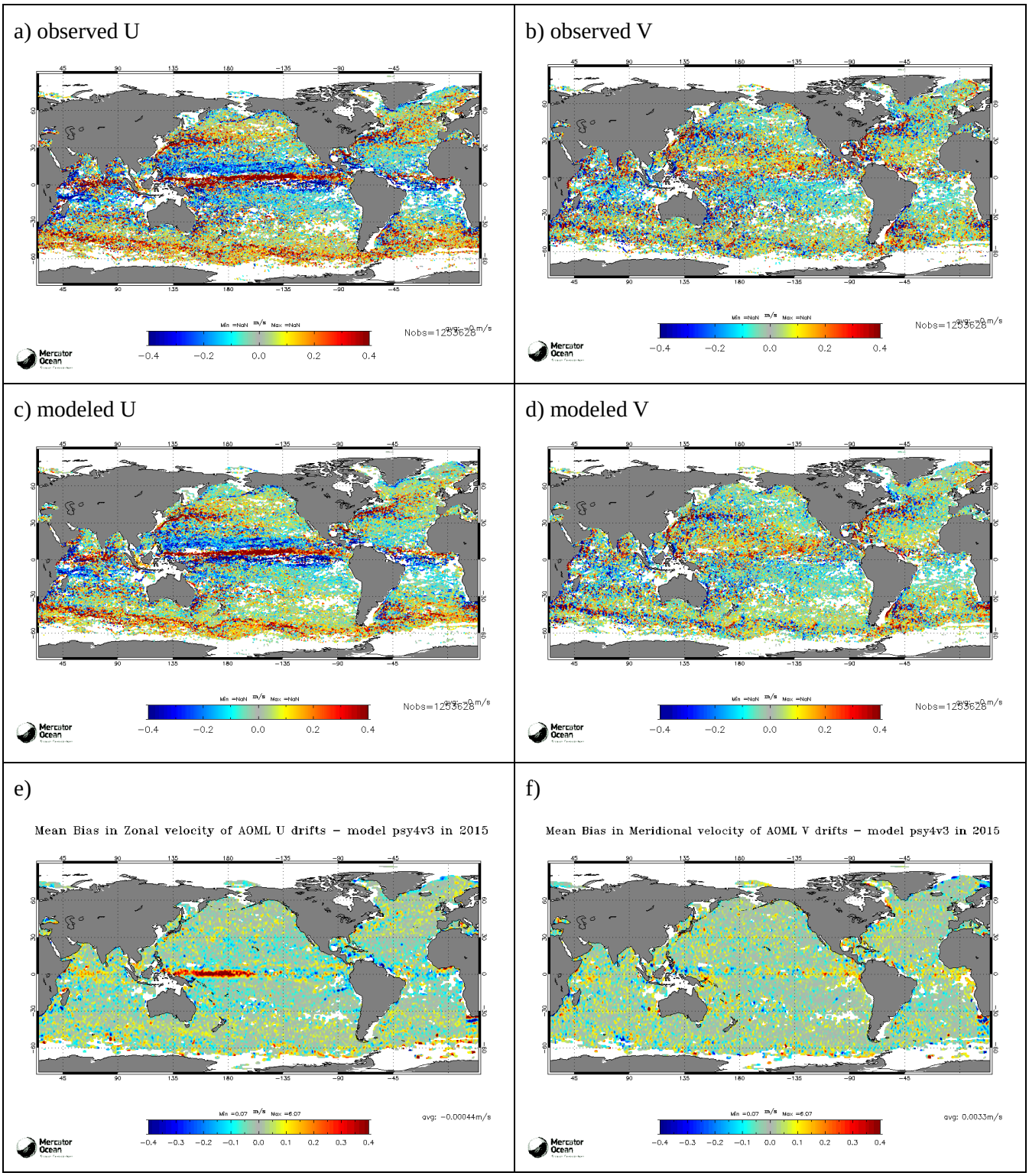

Figure 15: maps of all observations gathered in 2015 for zonal u (m/s, a) and meridional v (m/s, b) velocities from drifters and ARGO floats. C) and d) GLO_HR V2.3 analysis counterpart for a) and b) respectively. e) zonal

velocity bias (m/s) and f) meridional velocity bias (m/s) deduced from the differences between GLO_HR V2.3 and the observations.

III.1.7 Mixed Layer Depth

Large scale mixed layer depth features are captured by the GLO_HR system, as shown by Figure 16. We note the strong interannual signal taking place in the North Atlantic in 2013-2015, where a strong cold anomaly is observed.

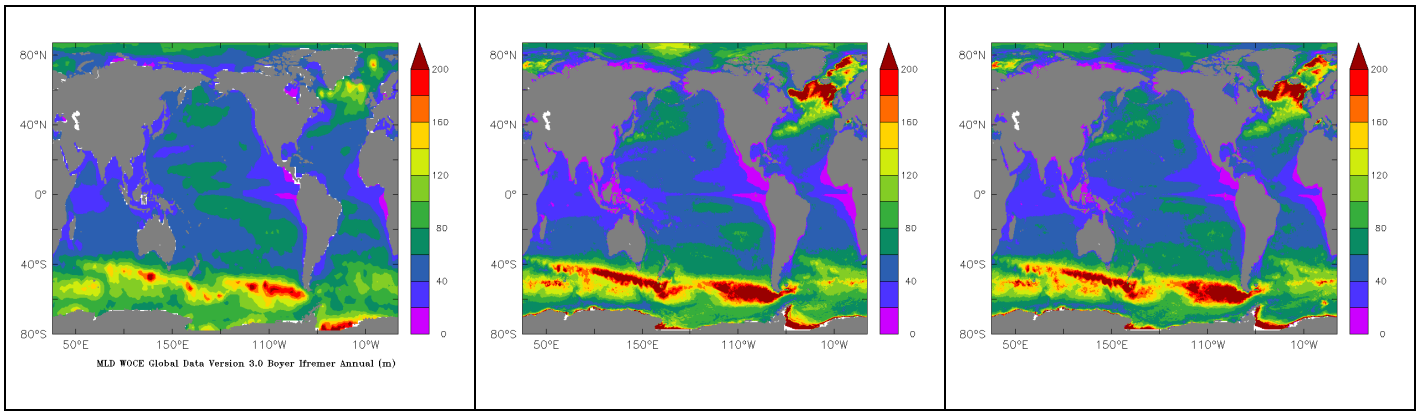

Figure 16 : climatological annual mean mixed layer depth (m). De Boyer Montegut climatology data (left) and GLO_HR-V2 (middle) (2013-2015 average) and GLO_HR V2.3 (right) (2013-2015 average).

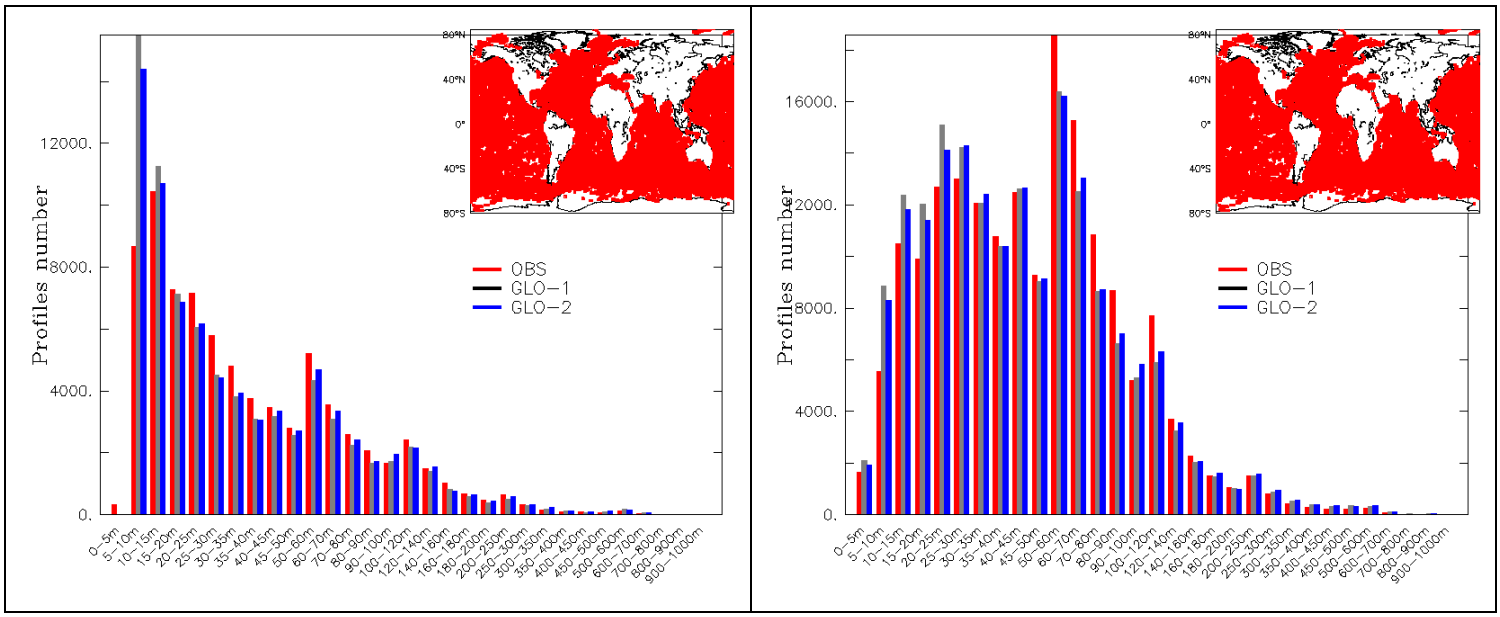

Figure 17 : 2015 distributions, for the global ocean, of Mixed Layer Depth, calculated from profiles with the density criteria (MLD defined as the depth at which density difference from the surface reaches 0.02 kg/m^3) (left) and temperature criteria (MLD defined as the depth at which temperature difference from the surface reaches 0.2°C)(right); V2 is in grey, V2.3 is in blue and the in situ observations in red.

Comparing the distributions of mixed layer depth at global scale in 2015 in Figure 17, we note that the density and temperature criteria give very different distributions, and that GLO_HR V2.3 is closer to observations than GLO_HR V2. In both V2 and V2.3, the mixed layer is too often shallower than in the observations.

EAN for this metric will be produced for V3.

III.1.8 Validation of high frequencies at tide-gauges

The GLO_HR system produces hourly outputs at the surface that can be compared with tide gauges measurements, from which we filter out the inverse barometer effect and the tides.

III.1.8.1 Sea surface Height

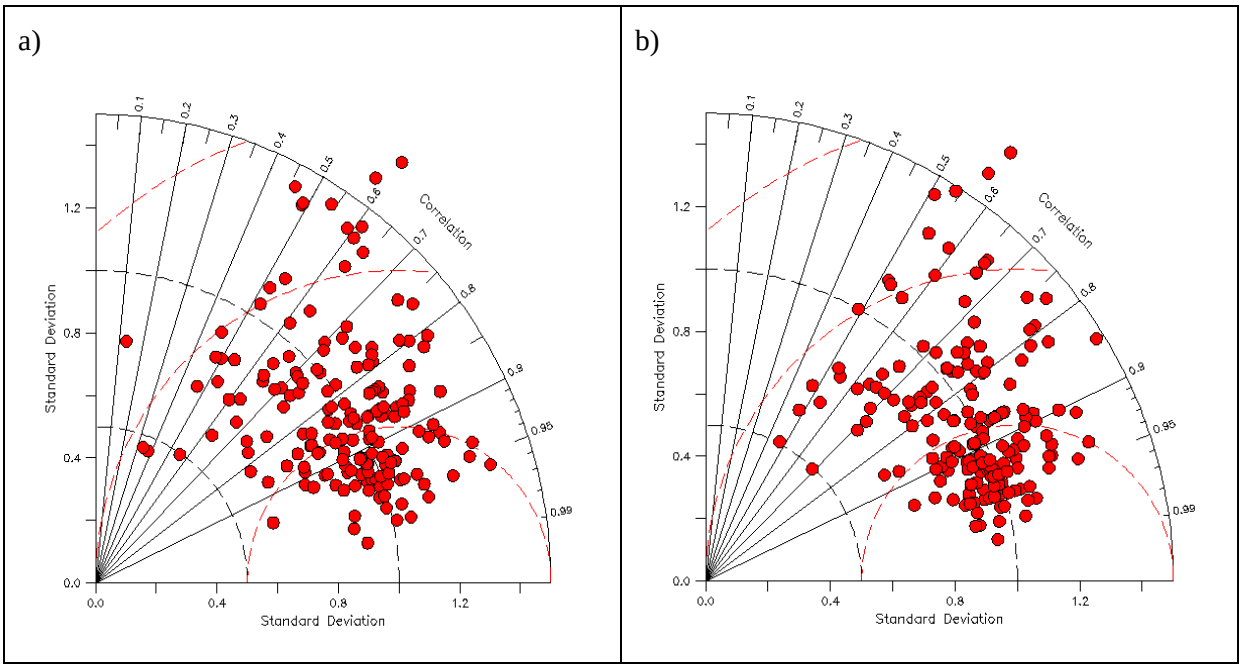

Figure 18 : Taylor diagram of the sea surface height errors (2015). Comparison between observations at tide gauges and GLO_HR systems. (a): GLO_HR V2. (b): GLO_HR V2.3.

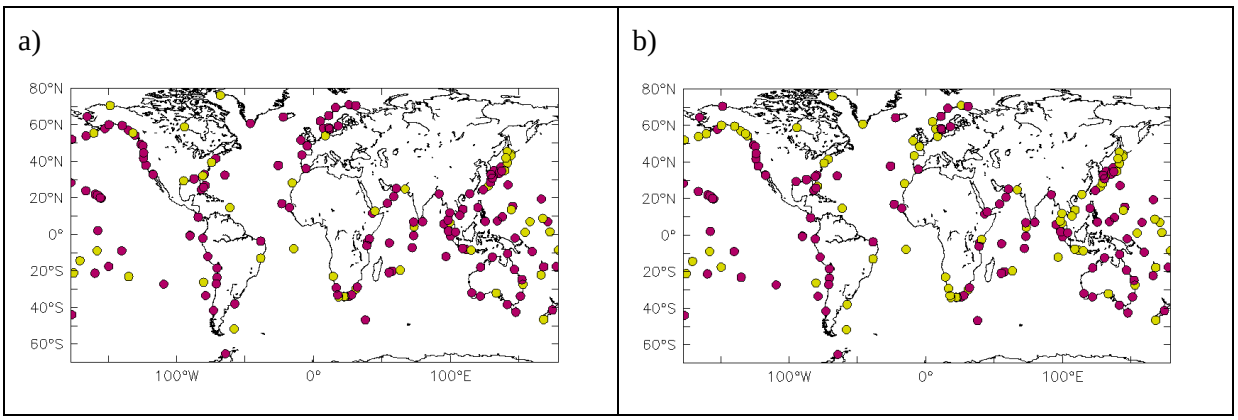

Figure 19 : comparison of the RMS difference (a) and the correlation (b) of the sea surface height between the observations at tide gauges and the V2.3 and v2 GLO_HR systems (2015). When the RMS difference (correlation) of GLO_HR V2.3 is lower (higher) than for GLO_HR v2, the color is red, otherwise it is yellow.

GLO_HR high frequency SSH (without tides or inverse barometer) compares well with tide gauges in many places, with a slight improvement in V2.3 with respect to V2, as shown by Figure 18, Figure 19 and Table 13.

Seal surface height (cm)	Hindcast				Forecast day 3			
	correlation		RMS of misfit		Mean misfit		RMS misfit	
	V2	V2.3	V2	V2.3	V2	V2.3	V2	V2.3
GLO	0.81	0.83	4.9	4.6	tbc	tbc	Tbc	tbc

Table 13: averaged values of RMS difference and correlation of the sea surface height in 2015

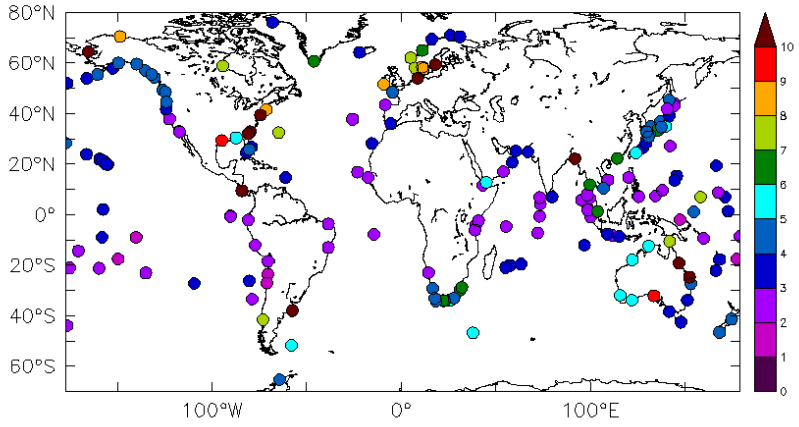

Figure 20 : Sea surface height RMS difference (cm) between observations at tide gauges and GLO_HR V2.3 for the year 2015.

The best agreement between GLO_HR and tide gauges is found in the tropical band, as can be seen in Figure 20, while shelf regions and closed seas are less accurate.

III.2 North Atlantic: NAT

III.2.1 Temperature

3D temperature accuracy results are synthesized in Table 14.

- Small biases (< 0.5K), reduced in subsurface from V2 to V2.3.
- RMS errors are large near the thermocline where the variability is higher. RMS is reduced in subsurface from V2 to V2.3.
- The modelled ocean surface is slightly too cold on average.
- The sub-surface ocean is generally warmer than the observations.
- Warm biases are found in the 2000-5000m layer but the statistics are not robust in this layer because of the fewer number of data.

3DT (K)	Hindcast				Forecast day 3			
	Mean misfit		RMS misfit		Mean misfit		RMS misfit	
	V2	V2.3	V2	V2.3	V2	V2.3	V2	V2.3
0-5m	0.01	0.04	0.91	1.01	tbc	tbc	tbc	tbc
5-100m	-0.09	-0.07	1.20	1.13	tbc	tbc	tbc	tbc
100-300m	-0.10	-0.06	0.92	0.88	tbc	tbc	tbc	tbc
300-800m	-0.05	-0.04	0.71	0.68	tbc	tbc	tbc	tbc
800-2000m	-0.02	-0.03	0.31	0.32	tbc	tbc	tbc	tbc
2000-5000m	-0.19	-0.10	0.33	0.28	tbc	tbc	tbc	tbc
0-5000m	-0.04	-0.04	0.60	0.58	tbc	tbc	tbc	tbc

Table 14: NAT RMS and average temperature misfits in K (observation-model) with respect to the CORIOLIS in situ observations, in contiguous layers from 0 to 5000m.

III.2.2 Salinity

3D salinity results are synthesized in Table 15.

- Small biases (< 0.1 psu).
- Salty bias at the surface.
- Mean error and RMS are significantly reduced in the 0-300m layer between V2 and V2.3.

3DS(PSU)	Hindcast				Forecast day 3			
	Mean misfit		RMS misfit		Mean misfit		RMS misfit	
	V2	V2.3	V2	V2.3	V2	V2.3	V2	V2.3
0-5m	-0.083	-0.039	0.389	0.250	tbc	tbc	tbc	tbc
5-100m	-0.035	0.003	0.304	0.202	tbc	tbc	tbc	tbc
100-300m	-0.010	-0.009	0.204	0.148	tbc	tbc	tbc	tbc
300-800m	-0.004	0.000	0.101	0.095	tbc	tbc	tbc	tbc
800-2000m	0.000	-0.003	0.049	0.049	tbc	tbc	tbc	tbc
2000-5000m	-0.015	-0.006	0.022	0.014	tbc	tbc	tbc	tbc
0-5000m	-0.004	-0.002	0.116	0.091	tbc	tbc	tbc	tbc

Table 15: NAT RMS and average salinity misfits in psu (observation-model) with respect to the CORIOLIS in situ observations, in contiguous layers from 0 to 5000m.

III.2.3 SLA

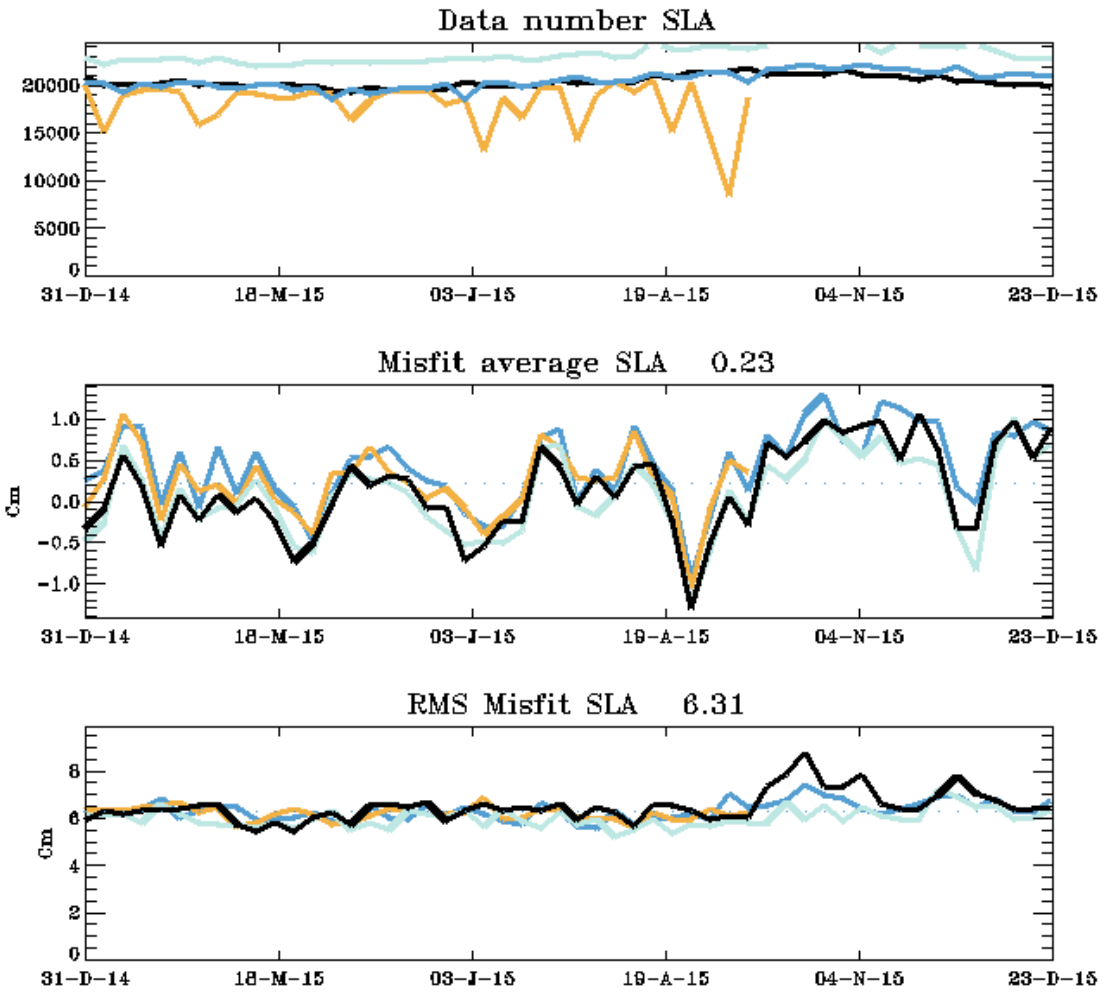

Figure 21: NAT RMS and average SLA misfits in cm (observation-model) with respect to all available altimetric missions in 2015 (black: Jason 2, cyan: SARAL/Altika, blue: HY-2, orange: Cryosat 2).

On average over the NAT zone (Table 16) we note a small positive observation – model anomaly of around 0.2 cm consistent with a cold bias. The RMS error is reduced of 1 cm on average from the previous version of the system to this new version.

Seal Level Anomaly (cm)	Hindcast				Forecast day 3			
	Mean misfit		RMS of misfit		Mean misfit		RMS misfit	
	V2	V2.3	V2	V2.3	V2	V2.3	V2	V2.3

NAT	-0.55	0.23	7.35	6.31	tbc	tbc	tbc	tbc

Table 16: NAT RMS and average SLA misfits in cm (observation-model) with respect to Jason 2, Saral/Altika and Cryosat2 observations. Statistics from the calibration period (year 2015) were used to build these regional estimates.

The stability over time of the GLO_HR system SLA statistics is illustrated inFigure 21, as well as the integration of all available observations (Jason 2, SARAL/Altika, HY-2, Cryosat 2).

III.3 Tropical Atlantic: TAT

III.3.1 Temperature

3D temperature accuracy results are synthesized in Table 17.

- Warm biases are detected in subsurface 0-800m layer.
- The warm surface bias is reduced from V2 to V2.3.
- RMS errors are large near the thermocline where the variability is higher, with a very slight increase from V2 to V2.3.

3DT (K)	**Hindcast**				**Forecast day 3**			
	Mean misfit		RMS misfit		Mean misfit		RMS misfit	
	V2	V2.3	V2	V2.3	V2	V2.3	V2	V2.3
0-5m	-0.10	-0.05	0.36	0.40	tbc	tbc	tbc	tbc
5-100m	-0.16	-0.19	1.01	1.10	tbc	tbc	tbc	tbc
100-300m	-0.11	-0.11	0.73	0.73	tbc	tbc	tbc	tbc
300-800m	-0.06	-0.06	0.50	0.51	tbc	tbc	tbc	tbc
800-2000m	0.00	0.01	0.09	0.12	tbc	tbc	tbc	tbc
2000-5000m	-0.06	-0.02	0.11	0.11	tbc	tbc	tbc	tbc
0-5000m	-0.03	-0.03	0.42	0.43	tbc	tbc	tbc	tbc

Table 17: TAT RMS and average temperature misfits in psu (observation-model) with respect to the CORIOLIS in situ observations, in contiguous layers from 0 to 5000m.

III.3.2 Salinity

3D salinity results are synthesized in Table 18.

- The fresh bias at the surface in the V2 system is four times smaller in V2.3 (now <0.03 psu on average over the basin).
- Biases and RMS errors are reduced in the 0-300m layer from V2 to V2.3.
- The bias is smaller but the RMS error slightly increases from V2 to V2.3 below 300 m depth.

3DS(PSU)	Hindcast				Forecast day 3			
	Mean misfit		RMS misfit		Mean misfit		RMS misfit	
	V2	V2.3	V2	V2.3	V2	V2.3	V2	V2.3
0-5m	0.119	0.029	0.403	0.229	tbc	tbc	tbc	tbc
5-100m	0.030	0.015	0.223	0.170	tbc	tbc	tbc	tbc
100-300m	-0.016	-0.012	0.117	0.114	tbc	tbc	tbc	tbc
300-800m	-0.004	-0.004	0.043	0.051	tbc	tbc	tbc	tbc
800-2000m	0.006	0.002	0.021	0.023	tbc	tbc	tbc	tbc
2000-5000m	0.001	0.000	0.013	0.021	tbc	tbc	tbc	tbc
0-5000m	0.003	0.000	0.068	0.061	tbc	tbc	tbc	tbc

Table 18: TAT RMS and average salinity misfits in psu (observation-model) with respect to the CORIOLIS in situ observations, in contiguous layers from 0 to 5000m.

III.3.3 SLA

V2.3 version reduces the RMS error by 0.5 cm with respect to V2, while the bias is slightly higher (0.04 cm) and is consistent with a fresh bias.

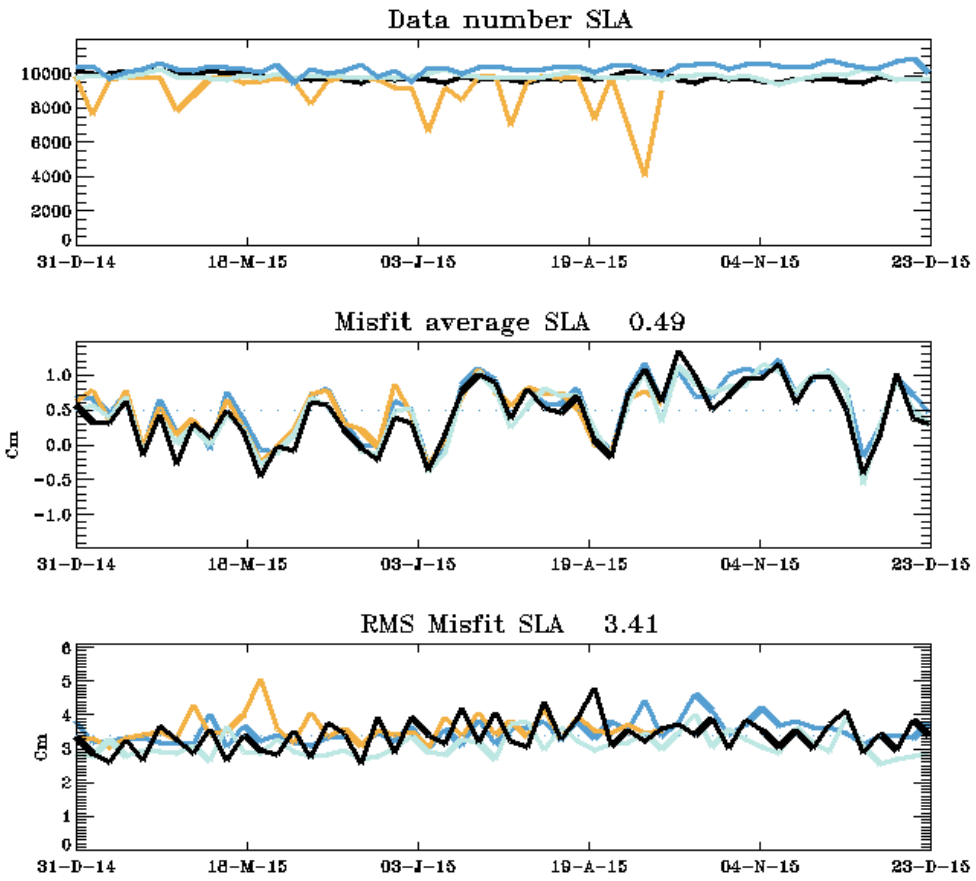

Figure 22: TAT RMS and average SLA misfits in cm (observation-model) with respect to all available altimetric missions in 2015 (black: Jason 2, cyan: SARAL/Altika, blue: HY-2, orange: Cryosat 2).

Seal Level Anomaly (cm)	Hindcast				Forecast day 3			
	Mean misfit		RMS misfit		Mean misfit		RMS misfit	
	V2	V2.3	V2	V2.3	V2	V2.3	V2	V2.3
TAT	0.45	0.49	4.03	3.41	tbc	tbc	Tbc	tbc

Table 19: TAT RMS and average SLA misfits in cm (observation-model) with respect to all available observations. Statistics from calibration period on year 2015 are used to build these regional estimates.

The stability over time of the GLO system SLA statistics in the TAT region is illustrated in Figure 22 as well as the integration of all available observations (Jason 2, SARAL/Altika, HY-2, Cryosat 2).

III.4 Mediterranean Sea: MED

III.4.1 Temperature

3D temperature accuracy results are synthesized in Table 20.

- The bias is cold at the surface (0.1K) and warm in subsurface layers below 100m (<0.05K).
- RMS errors are slightly higher in V2.3 at the surface.
- RMS errors are larger in the 2000-5000m layer in V2.3, but results are not robust in this layer where very few observations are available, further monitoring of these errors is necessary.

3DT (K)	Hindcast				Forecast day 3			
	Mean misfit		RMS misfit		Mean misfit		RMS misfit	
	V2	V2.3	V2	V2.3	V2	V2.3	V2	V2.3
0-5m	0.05	0.11	0.65	0.79	tbc	tbc	tbc	tbc
5-100m	-0.04	-0.07	0.80	0.80	tbc	tbc	tbc	tbc
100-300m	-0.02	-0.04	0.30	0.30	tbc	tbc	tbc	tbc
300-800m	0.04	0.00	0.18	0.17	tbc	tbc	tbc	tbc
800-2000m	-0.01	-0.01	0.09	0.08	tbc	tbc	tbc	tbc
2000-5000m	0.05	0.09	0.09	0.57	tbc	tbc	tbc	tbc
0-5000m	0.00	-0.01	0.26	0.26	tbc	tbc	tbc	tbc

Table 20: MED RMS and average temperature misfits in K (observation-model) with respect to the CORIOLIS in situ observations, in contiguous layers from 0 to 5000m.

III.4.2 Salinity

3D salinity results are synthesized in Table 21.

- Small biases (< 0.05 psu).
- V2.3 biases smaller than V2 in the 0-100m layer but higher in the 100-800m layer.
- Surface RMS error decreases of ~ 0.15 psu over the domain in V2.3 with respect to V2.

3DS(PSU)	Hindcast				Forecast day 3			
	Mean misfit		RMS misfit		Mean misfit		RMS misfit	
	V2	V2.3	V2	V2.3	V2	V2.3	V2	V2.3
0-5m	0.084	-0.009	0.393	0.258	Tbc	tbc	tbc	tbc
5-100m	0.074	0.030	0.273	0.199	Tbc	tbc	tbc	tbc
100-300m	0.003	-0.003	0.112	0.102	Tbc	tbc	tbc	tbc
300-800m	0.003	0.005	0.044	0.044	Tbc	tbc	tbc	tbc

800-2000m	-0.004	-0.003	0.029	0.029	Tbc	tbc	tbc	tbc
2000-5000m	0.000	-0.025	0.016	0.044	Tbc	tbc	tbc	tbc
0-5000m	0.004	0.002	0.087	0.071	Tbc	tbc	tbc	tbc

Table 21 : MED RMS and average salinity misfits in PSU (observation-model) with respect to the CORIOLIS in situ observations, in contiguous layers from 0 to 5000m.

III.4.3 SLA

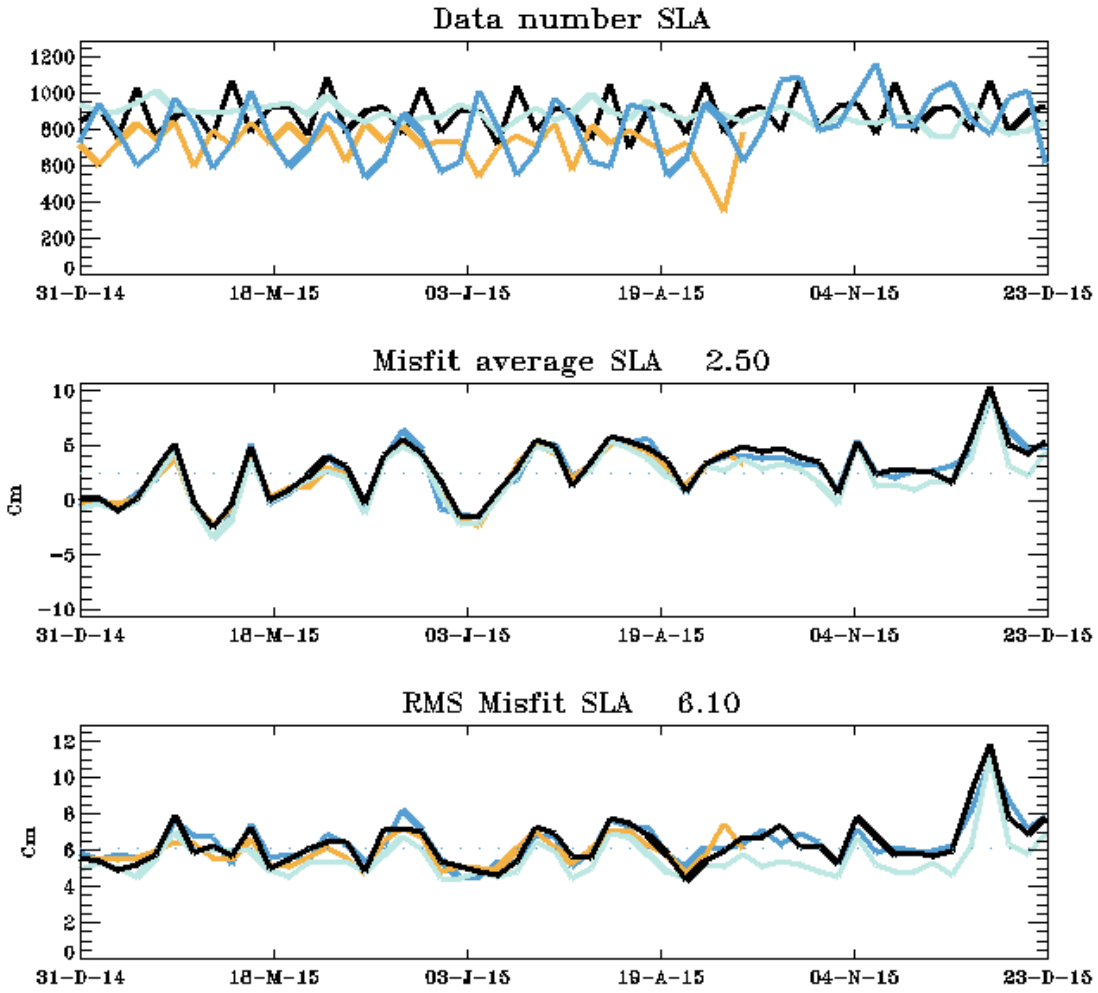

Figure 23: MED RMS and average SLA misfits in cm (observation-model) with respect to all available altimetric missions in 2015 (black: Jason 2, cyan: SARAL/Altika, blue: HY-2, orange: Cryosat 2).

Seal Level Anomaly (cm)	**Hindcast**				**Forecast day 3**			
	Mean misfit		RMS misfit		Mean misfit		RMS misfit	
	V2	V2.3	V2	V2.3	V2	V2.3	V2	V2.3

MED	2.26	2.50	8.59	6.10	tbc	tbc	tbc	tbc

Table 22: MED RMS and average SLA misfits in cm (observation-model) with respect to all available observations. Statistics from calibration period on year 2015 are used to build these regional estimates.

The SLA bias is more important in the MED region than in the Atlantic, and stays below 3 cm on average (Figure 23). This high value is due to strong biases of more than 3 cm in the Ionian Sea and Sicily regions (not shown). These regions are shallow and close to the coast. As a consequence, the SLA observation error is high in these zones in GLO_HR. Thus, these regions are poorly constrained and biases are observed.

III.5 South Atlantic: SAT

III.5.1 Temperature

3D temperature accuracy results are synthesized in Table 23.

- Warm biases are found from the surface to 800m (~0.1K).
- RMS errors are large near the thermocline where the variability is higher.
- Mean and RMS errors slightly increase from V2 to V2.3.

3DT (K)	Hindcast				Forecast day 3			
	Mean misfit		RMS misfit		Mean misfit		RMS misfit	
	V2	V2.3	V2	V2.3	V2	V2.3	V2	V2.3
0-5m	-0.07	-0.09	0.54	0.62	tbc	tbc	tbc	tbc
5-100m	-0.09	-0.14	0.87	0.92	tbc	tbc	tbc	tbc
100-300m	-0.10	-0.14	0.77	0.75	tbc	tbc	tbc	tbc
300-800m	-0.04	-0.06	0.46	0.48	tbc	tbc	tbc	tbc
800-2000m	0.01	0.01	0.15	0.15	tbc	tbc	tbc	tbc
2000-5000m	-0.03	0.04	0.12	0.20	tbc	tbc	tbc	tbc
0-5000m	-0.02	-0.03	0.40	0.41	tbc	tbc	tbc	tbc

Table 23: SAT RMS and average temperature misfits in K (observation-model) with respect to the CORIOLIS in situ observations, in contiguous layers from 0 to 5000m.

III.5.2 Salinity

3D salinity results are synthesized in Table 24.

- Small biases (< 0.01PSU) reduced from V2 to V2.3.
- Small rms error (<0.2 PSU) reduced from V2 to V2.3.

- RMS errors are large in the surface layer and near the thermocline where the variability is higher.

3DS(PSU)	Hindcast				Forecast day 3			
	Mean misfit		RMS misfit		Mean misfit		RMS misfit	
	V2	V2.3	V2	V2.3	V2	V2.3	V2	V2.3
0-5m	0.048	0.002	0.274	0.182	tbc	tbc	tbc	tbc
5-100m	0.013	0.002	0.180	0.146	tbc	tbc	tbc	tbc
100-300m	-0.007	-0.011	0.128	0.121	tbc	tbc	tbc	tbc
300-800m	0.000	-0.002	0.063	0.064	tbc	tbc	tbc	tbc
800-2000m	0.005	0.004	0.026	0.028	tbc	tbc	tbc	tbc
2000-5000m	0.005	-0.001	0.015	0.018	tbc	tbc	tbc	tbc
0-5000m	0.003	0.001	0.068	0.063	tbc	tbc	tbc	tbc

Table 24: SAT RMS and average salinity misfits in PSU (observation-model) with respect to the CORIOLIS in situ observations, in contiguous layers from 0 to 5000m.

III.5.3 SLA

As can be seen in Table 25 and Figure 24, the forecast is close to the SLA observations. A positive observation – model misfit of 1cm (consistent with a cold bias) can be diagnosed, while the RMS error is less than 7 cm. The RMS error is slightly lower is the V2.3 version than in V2.

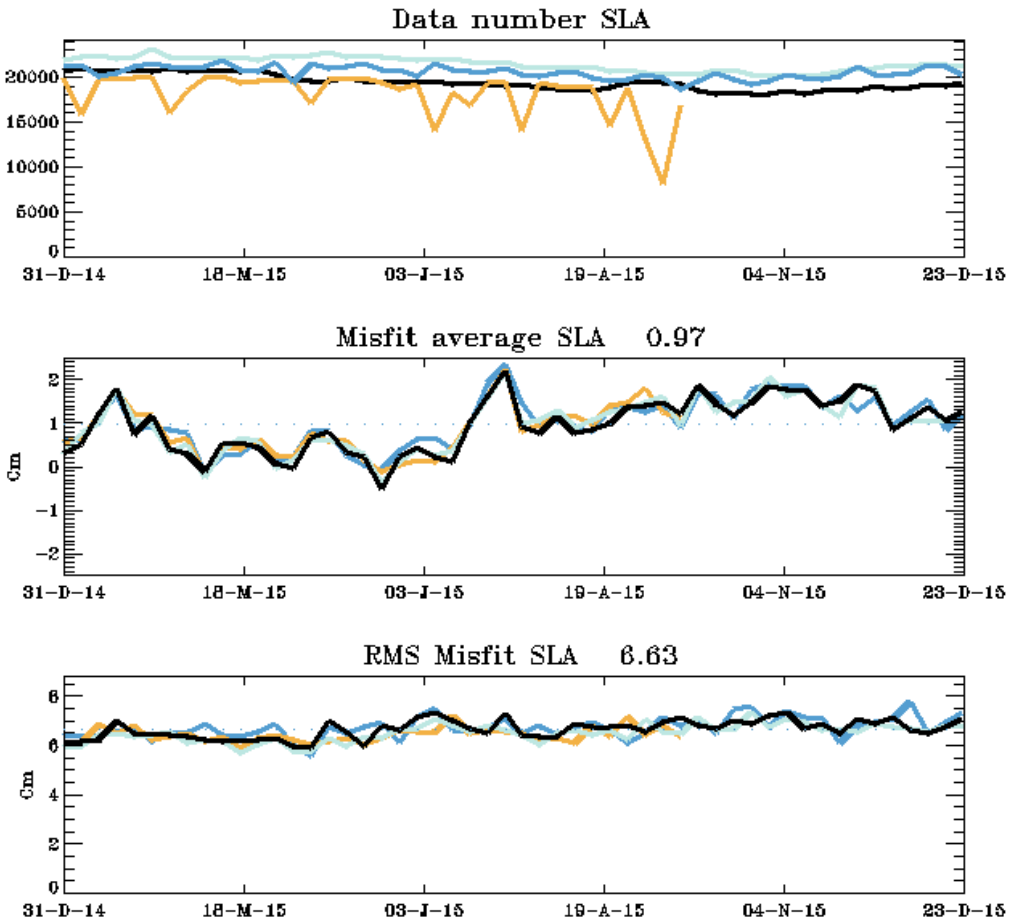

Figure 24: SAT RMS and average SLA misfits in cm (observation-model) with respect to all available altimetric missions in 2015 (black: Jason 2, cyan: SARAL/Altika, blue: HY-2, orange: Cryosat 2).

Seal Level Anomaly (cm)	Hindcast				Forecast day 3			
	Mean misfit		RMS misfit		Mean misfit		RMS misfit	
	V2	V2.3	V2	V2.3	V2	V2.3	V2	V2.3
SAT	0.78	0.97	6.80	6.63	tbc	tbc	tbc	tbc

Table 25: SAT RMS and average SLA misfits in cm (observation-model) with respect to all available altimetric missions in 2015.

The stability over time of the GLO system SLA statistics in the SAT region is illustrated in Figure 24 as well as the integration of all available observations (MyOcean V4 observations, SARAL/Altika, HY-2, Cryosat 2).

III.6 Indian Ocean: IND

III.6.1 Temperature

3D temperature accuracy results are synthesized in Table 26.

- Biases are reduced from V2 to V2.3 in the whole water column (<0.05 K).
- Rms error slightly increases from V2 to V2.3 over the whole water column (<0.1 K).
- RMS errors are large near the thermocline where the variability is higher.

3DT (K)	Hindcast				Forecast day 3			
	Mean misfit		RMS misfit		Mean misfit		RMS misfit	
	V2	V2.3	V2	V2.3	V2	V2.3	V2	V2.3
0-5m	-0.04	0.02	0.40	0.44	tbc	tbc	tbc	tbc
5-100m	0.10	-0.03	0.87	0.92	tbc	tbc	tbc	tbc
100-300m	0.03	-0.03	0.73	0.85	tbc	tbc	tbc	tbc
300-800m	0.00	0.00	0.29	0.35	tbc	tbc	tbc	tbc
800-2000m	0.01	0.00	0.18	0.23	tbc	tbc	tbc	tbc
2000-5000m	0.03	0.07	0.03	0.07	tbc	tbc	tbc	tbc
0-5000m	0.01	0.00	0.36	0.41	tbc	tbc	tbc	tbc

Table 26: IND RMS and average temperature misfits in K (observation-model) with respect to the CORIOLIS in situ observations, in contiguous layers from 0 to 5000m.

III.6.2 Salinity

3D salinity results are synthesized in Table 27.

- A fresh bias is found at the surface, but has been slightly reduced from V2 to V2.3 (<0.03 psu).
- Biases were reduced from V2 to V2.3 in subsurface.
- Biases increase under 2000m but may not be robust (too few observations).
- RMS error reduced from V2 to V2.3 in the 0-300 m layer (<0.2).

3DS(PSU)	Hindcast				Forecast day 3			
	Mean misfit		RMS misfit		Mean misfit		RMS misfit	
	V2	V2.3	V2	V2.3	V2	V2.3	V2	V2.3
0-5m	0.039	0.026	0.240	0.204	tbc	Tbc	tbc	tbc
5-100m	-0.008	0.008	0.182	0.168	tbc	Tbc	tbc	tbc
100-300m	-0.004	0.000	0.094	0.096	tbc	Tbc	tbc	tbc
300-800m	0.001	0.002	0.047	0.054	tbc	Tbc	tbc	tbc
800-2000m	0.001	0.001	0.026	0.033	tbc	Tbc	tbc	tbc

2000-5000m	-0.008	-0.029	0.008	0.029	tbc	Tbc	tbc	tbc
0-5000m	0.000	0.001	0.058	0.060	tbc	Tbc	tbc	tbc

Table 27: IND RMS and average salinity misfits in PSU (observation-model) with respect to the CORIOLIS in situ observations, in contiguous layers from 0 to 5000m.

III.6.3 SLA

The SLA bias is close to zero or negative in the Indian ocean, as seen in Figure 25 and Table 28.The RMS error is around 5 cm. The V2.3 version performs better than V2 in RMS and Average misfit.

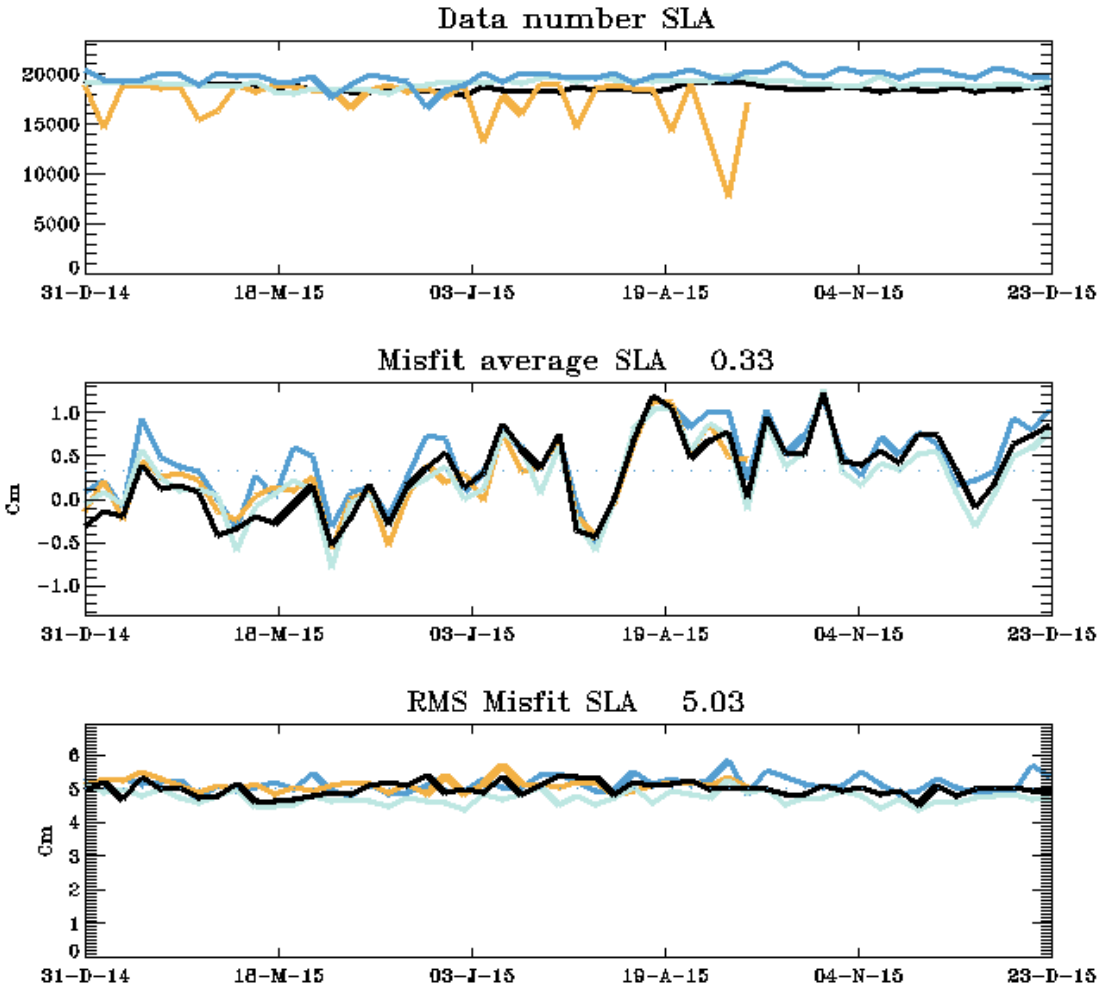

Figure 25: IND RMS and average SLA misfits in cm (observation-model) with respect to all available altimetric missions in 2015 (black: Jason 2, cyan: SARAL/Altika, blue: HY-2, orange: Cryosat 2).

Seal Level Anomaly	Hindcast		Forecast day 3	
	Mean misfit	RMS misfit	Mean misfit	RMS misfit

(cm)	V2	V2.3	V2	V2.3	V2	V2.3	V2	V2.3
IND	0.09	0.33	5.59	5.03	Tbc	tbc	tbc	tbc

Table 28: IND RMS and average SLA misfits in cm (observation-model) with respect to all available altimetric missions in 2015.

The stability over time of the GLO system SLA statistics in the IND region is illustrated in Figure 25**Erreur ! Source du renvoi introuvable.**, as well as the integration of all available observations (MyOcean V4 observations, SARAL/Altika, HY-2, Cryosat 2).

III.7 Arctic Ocean: ARC

III.7.1 Temperature

3D temperature accuracy results are synthesized in Table 29.

- The cold bias at the surface increases from V2 to V2.3 (0.16 K).
- Biases reduced from V2 to V2.3 in the whole water column (<0.1 K).
- RMS error reduced from V2 to V2.3 in subsurface under 100 m (<0.5 K).

However one must keep in mind that very few in situ observations are available to constrain the systems in this region.

3DT (K)	Hindcast				Forecast day 3			
	Mean misfit		RMS misfit		Mean misfit		RMS misfit	
	V2	V2.3	V2	V2.3	V2	V2.3	V2	V2.3
0-5m	0.10	0.16	0.83	0.89	tbc	tbc	tbc	tbc
5-100m	-0.05	0.00	0.65	0.66	tbc	tbc	tbc	tbc
100-300m	-0.06	0.04	0.49	0.46	tbc	tbc	tbc	tbc
300-800m	-0.03	0.00	0.39	0.36	tbc	tbc	tbc	tbc
800-2000m	-0.03	-0.02	0.25	0.23	tbc	tbc	tbc	tbc
2000-5000m	-0.13	-0.08	0.38	0.29	tbc	tbc	tbc	tbc
0-5000m	-0.03	-0.01	0.36	0.35	tbc	tbc	tbc	tbc

Table 29: ARC RMS and average temperature misfits in K (observation-model) with respect to the CORIOLIS in situ observations, in contiguous layers from 0 to 5000m.

III.7.2 Salinity

3D salinity results are synthesized in Table 30.

- A salty bias is diagnosed at the surface (<0.1 psu) and a small fresh bias in the 100-300 m layer (around 0.01 psu)
- RMS error is reduced in the V2.3 version with respect to the V2

3DS(PSU)	Hindcast				Forecast day 3			
	Mean misfit		RMS misfit		Mean misfit		RMS misfit	
	V2	V2.3	V2	V2.3	V2	V2.3	V2	V2.3
0-5m	-0.143	-0.062	0.397	0.248	tbc	tbc	tbc	tbc
5-100m	-0.064	-0.007	0.409	0.201	tbc	tbc	tbc	tbc
100-300m	0.017	0.014	0.190	0.127	tbc	tbc	tbc	tbc
300-800m	-0.004	0.000	0.039	0.035	tbc	tbc	tbc	tbc
800-2000m	-0.004	-0.002	0.024	0.023	tbc	tbc	tbc	tbc
2000-5000m	-0.004	-0.002	0.017	0.010	tbc	tbc	tbc	tbc
0-5000m	-0.005	0.000	0.122	0.070	tbc	tbc	tbc	tbc

Table 30: ARC RMS and average salinity misfits in psu (observation-model) with respect to the CORIOLIS in situ observations, in contiguous layers from 0 to 5000m.

III.7.3 SLA

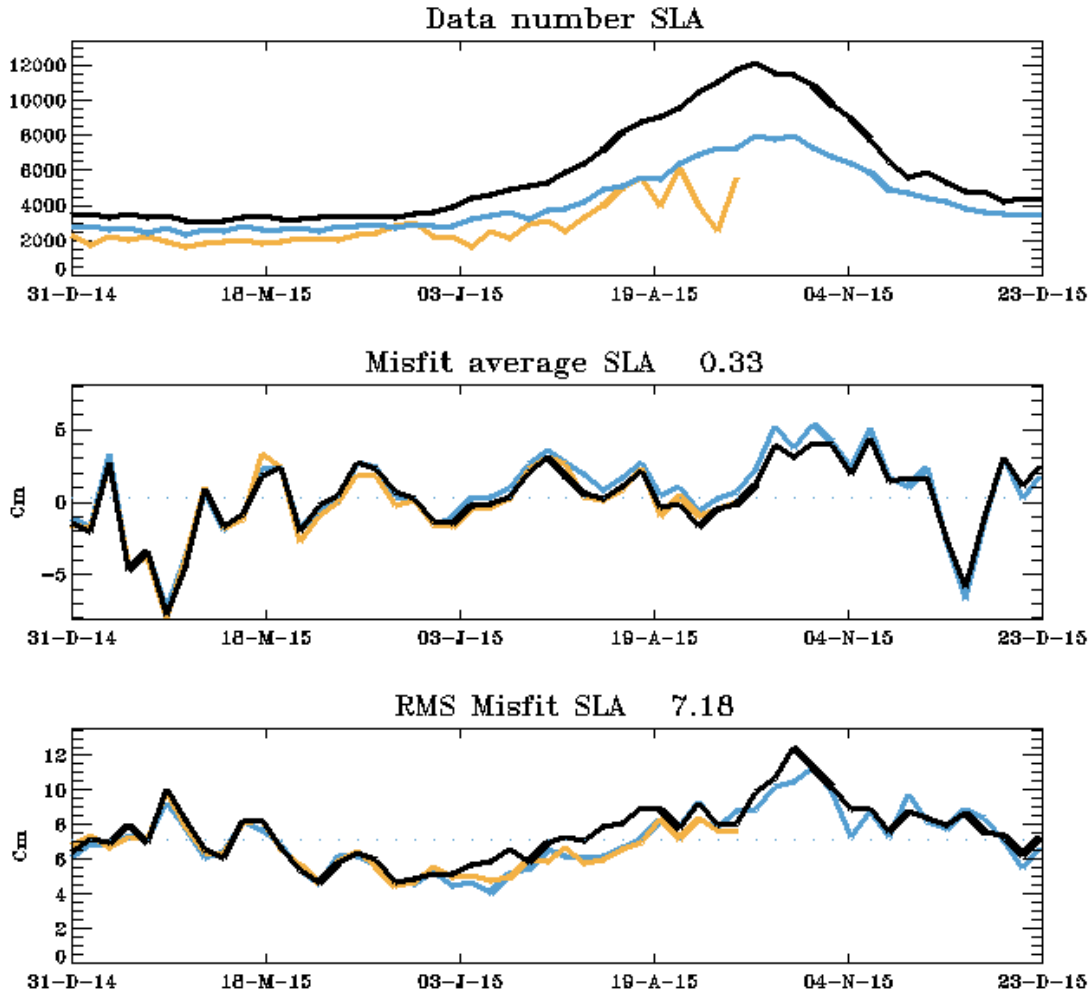

Figure 26: ARC RMS and average SLA misfits in cm (observation-model) with respect to all available altimetric missions in 2015 (black: Jason 2, cyan: SARAL/Altika, blue: HY-2, orange: Cryosat 2).

Seal Level Anomaly (cm)	Hindcast				Forecast day 3			
	RMS of misfit		Average misfit		RMS of misfit		Average misfit	
	V2	V2.3	V2	V2.3	V2	V2.3	V2	V2.3
ARC	8.98	7.18	-3.42	0.33	tbc	tbc	tbc	tbc

Table 31: ARC RMS and average SLA misfits in cm (observation-model) with respect to all available altimetric missions in 2015.

Some SLA observations are available in 2014 in the Arctic as can be seen in Figure 26**Erreur ! Source du renvoi introuvable.**. However, the average misfist and RMS misfit may not be representative of the Arctic Ocean because the mean dynamic topography has many errors in this region, and because of the very variable extent of the coverage due to seasonal sea ice.

III.7.4 Sea ice variables

Please refer to Table 12.

III.8 Southern Ocean: ACC

III.8.1 Temperature

3D temperature accuracy results are synthesized in Table 32.

- Mean misfit slightly increases in the V2.3 version with respect to the V2 version.
- RMS errors slightly increase near the surface and below 800m depth.
- RMS errors are around 0.6 K on average in the 0-300m layer and slightly decrease with respect to V2.

3DT (K)	Hindcast				Forecast day 3			
	Mean misfit		RMS misfit		Mean misfit		RMS misfit	
	V2	V2.3	V2	V2.3	V2	V2.3	V2	V2.3
0-5m	0.01	-0.03	0.54	0.57	tbc	tbc	tbc	tbc
5-100m	-0.01	-0.05	0.57	0.53	tbc	tbc	tbc	tbc
100-300m	-0.09	-0.09	0.63	0.57	tbc	tbc	tbc	tbc
300-800m	-0.04	-0.06	0.40	0.40	tbc	tbc	tbc	tbc
800-2000m	-0.01	-0.01	0.13	0.14	tbc	tbc	tbc	tbc
2000-5000m	-0.02	0.05	0.07	0.08	tbc	tbc	tbc	tbc
0-5000m	-0.02	-0.03	0.33	0.32	tbc	tbc	tbc	tbc

Table 32: ACC RMS and average temperature misfits in K (observation-model) with respect to the CORIOLIS in situ observations, in contiguous layers from 0 to 5000m.

III.8.2 Salinity

3D salinity results are synthesized in Table 33.

- Very small biases are found (< 0.02 psu), which slightly increase in V2.3 with respect to V2 in subsurface.
- Very small RMS error are found (< 0.15 psu), with improvement in V2.3 on the 0-800 m layer.

3DS(PSU)	Hindcast				Forecast day 3			
	Mean misfit		RMS misfit		Mean misfit		RMS misfit	
	V2	V2.3	V2	V2.3	V2	V2.3	V2	V2.3

0-5m	0.004	0.003	0.172	0.125	tbc	tbc	tbc	tbc
5-100m	0.006	0.012	0.148	0.120	tbc	tbc	tbc	tbc
100-300m	0.001	0.002	0.103	0.095	tbc	tbc	tbc	tbc
300-800m	0.002	0.003	0.061	0.055	tbc	tbc	tbc	tbc
800-2000m	0.003	0.004	0.021	0.021	tbc	tbc	tbc	tbc
2000-5000m	-0.008	-0.007	0.010	0.010	tbc	tbc	tbc	tbc
0-5000m	0.003	0.004	0.058	0.051	tbc	tbc	tbc	tbc

Table 33: ACC RMS and average salinity misfits in psu (observation-model) with respect to the CORIOLIS in situ observations, in contiguous layers from 0 to 5000m.

III.8.3 SLA

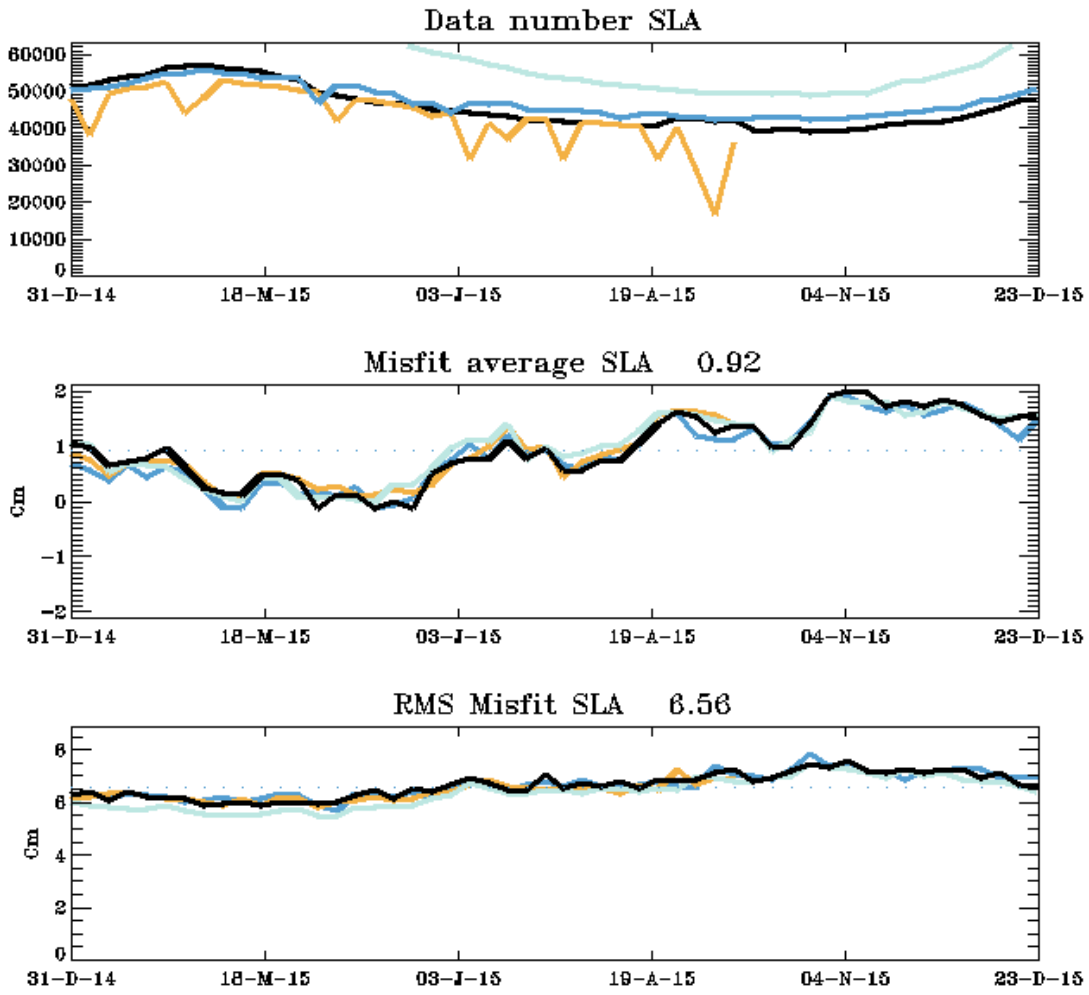

Figure 27: ACC RMS and average SLA misfits in cm (observation-model) with respect to all available altimetric missions in 2015 (black: Jason 2, cyan: SARAL/Altika, blue: HY-2, orange: Cryosat 2).

Seal Level Anomaly (cm)	Hindcast				Forecast day 3			
	Mean misfit		RMS misfit		Mean misfit		RMS misfit	
	V2	V2.3	V2	V2.3	V2	V2.3	V2	V2.3
ACC	1.05	0.92	8.98	6.56	tbc	tbc	tbc	tbc

Table 34: ACC RMS and average SLA misfits in cm (observation-model) with respect to all available altimetric missions in 2015

As can be seen in Table 34 the average (< 1cm) and RMS misfit (< 7 cm) in the ACC have decreased in V2.3 with respect to V2, with a 2 cm improvement in RMS error.

III.8.4 Sea ice variables

Please refer to Table 12.

III.9 South Pacific Ocean: SPA

III.9.1 Temperature

3D temperature accuracy results are synthesized in Table 35.

- Warm biases are found from the surface down to 800m (~0.1 K), increasing in V2.3 with respect to V2.
- RMS errors are large near the thermocline where the variability is higher (up to 0.8K).
- RMS slightly increasing from V2 to V2.

3DT (K)	Hindcast				Forecast day 3			
	Mean misfit		RMS misfit		Mean misfit		RMS misfit	
	V2	V2.3	V2	V2.3	V2	V2.3	V2	V2.3
0-5m	-0.03	-0.12	0.41	0.53	tbc	tbc	tbc	tbc
5-100m	0.00	-0.06	0.61	0.68	tbc	tbc	tbc	tbc
100-300m	-0.07	-0.09	0.68	0.76	tbc	tbc	tbc	tbc
300-800m	-0.03	-0.04	0.32	0.35	tbc	tbc	tbc	tbc
800-2000m	0.00	0.00	0.10	0.11	tbc	tbc	tbc	tbc
2000-5000m	-0.01	0.04	0.05	0.07	tbc	tbc	tbc	tbc
0-5000m	-0.01	-0.02	0.31	0.34	tbc	tbc	tbc	tbc

Table 35: SPA RMS and average temperature misfits in K (observation-model) with respect to the CORIOLIS in situ observations, in contiguous layers from 0 to 5000m.

III.9.2 Salinity

3D salinity results are synthesized in Table 36.

- Biases are reduced in V2.3 over the whole water column.
- RMS error were slightly reduced from V2 to V2.3 over the whole water column (<0.15 psu).

3DS(PSU)	Hindcast				Forecast day 3			
	RMS of misfit		Average misfit		RMS of misfit		Average misfit	
	V2	V2.3	V2	V2.3	V2	V2.3	V2	V2.3
0-5m	0.016	0.007	0.150	0.145	tbc	tbc	tbc	tbc
5-100m	0.002	0.002	0.127	0.125	tbc	tbc	tbc	tbc
100-300m	-0.006	-0.002	0.091	0.090	tbc	tbc	tbc	tbc
300-800m	-0.002	-0.001	0.036	0.039	tbc	tbc	tbc	tbc
800-2000m	0.001	0.001	0.013	0.015	tbc	tbc	tbc	tbc
2000-5000m	-0.002	-0.005	0.008	0.009	tbc	tbc	tbc	tbc
0-5000m	0.000	0.000	0.045	0.045	tbc	tbc	tbc	tbc

Table 36: SPA RMS and average salinity misfits in psu (observation-model) with respect to the CORIOLIS in situ observations, in contiguous layers from 0 to 5000m.

III.9.3 SLA

The SLA bias in SPA is very small (<0.1 cm on average) while the RMS error is 5 cm on average, which shows an overall improvement with respect to V2 (Table 37).

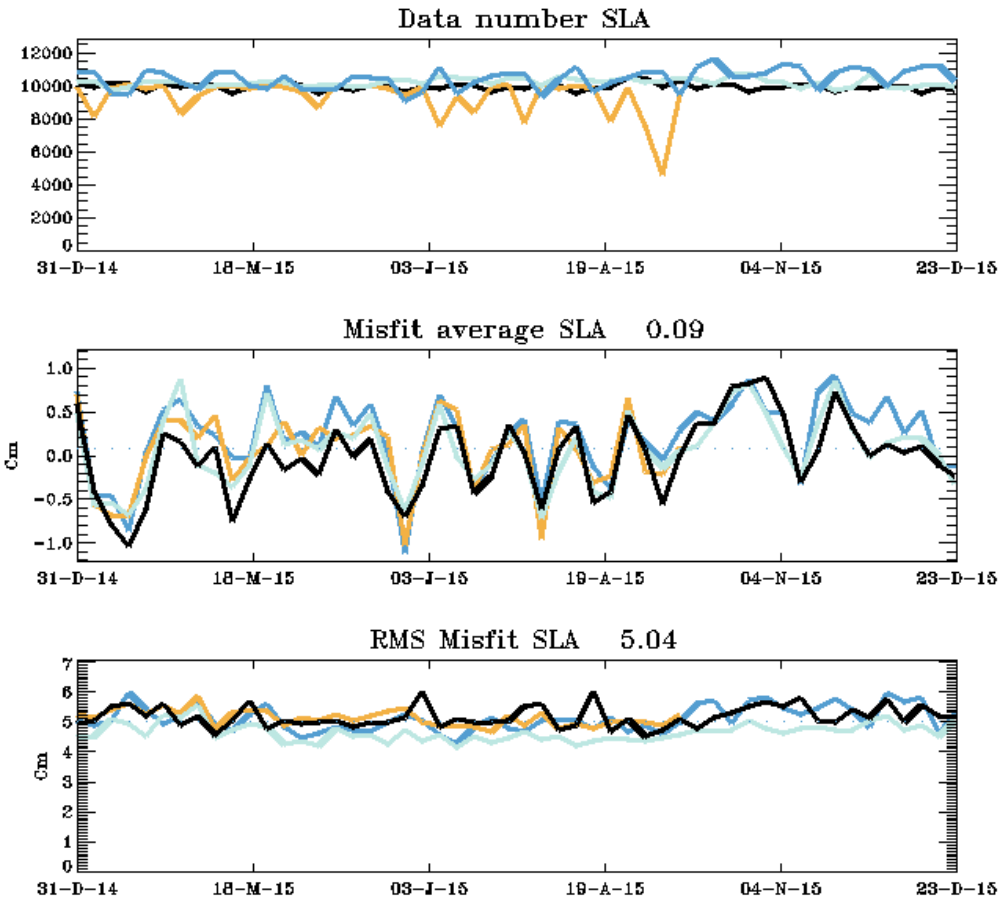

Figure 28: SPA RMS and average SLA misfits in cm (observation-model) with respect to all available altimetric missions in 2015 (black: Jason 2, cyan: SARAL/Altika, blue: HY-2, orange: Cryosat 2).

Seal Level Anomaly (cm)	Hindcast				Forecast day 3			
	Mean misfit		RMS misfit		Mean misfit		RMS misfit	
	V2	V2.3	V2	V2.3	V2	V2.3	V2	V2.3
SPA	-0.43	0.09	6.46	5.04	tbc	tbc	tbc	tbc

Table 37: SPA RMS and average SLA misfits in cm (observation-model) with respect to all available altimetric missions in 2015

III.10 Tropical Pacific Ocean: TPA

III.10.1 Temperature

3D temperature accuracy results are synthesized in Table 38.

- Warm biases are found from the surface down to 100m (0.15K at the surface and 0.05K in subsurface waters).
- RMS errors increase from V2 to V2.3 in the whole water column (~0.9K in the thermocline).

3DT (K)	Hindcast				Forecast day 3			
	Mean misfit		RMS misfit		Mean misfit		RMS misfit	
	V2	V2.3	V2	V2.3	V2	V2.3	V2	V2.3
0-5m	-0.05	-0.15	0.36	0.50	tbc	tbc	tbc	tbc
5-100m	0.03	-0.05	0.82	0.91	tbc	tbc	tbc	tbc
100-300m	-0.04	-0.06	0.79	0.89	tbc	tbc	tbc	tbc
300-800m	-0.01	-0.02	0.29	0.33	tbc	tbc	tbc	tbc
800-2000m	0.00	0.01	0.09	0.11	tbc	tbc	tbc	tbc
2000-5000m	-0.01	0.03	0.05	0.07	tbc	tbc	tbc	tbc
0-5000m	0.00	-0.01	0.34	0.39	tbc	tbc	tbc	tbc

Table 38: TPA RMS and average temperature misfits in K (observation-model) with respect to the CORIOLIS in situ observations, in contiguous layers from 0 to 5000m.

III.10.2 Salinity

3D salinity results are synthesized in Table 39.

- Fresh biases are found from the surface down to 100m (up to 0.02 PSU).
- Biases and RMS were reduced from V2 to V2.3 on the 0-100m.
- equivalent performance (or slight degradation) under 300m between V2 and V2.3.

3DS(PSU)	Hindcast				Forecast day 3			
	Mean misfit		RMS misfit		Mean misfit		RMS misfit	
	V2	V2.3	V2	V2.3	V2	V2.3	V2	V2.3
0-5m	0.029	0.019	0.197	0.188	tbc	tbc	tbc	tbc
5-100m	-0.006	0.001	0.174	0.167	tbc	tbc	tbc	tbc
100-300m	-0.005	-0.001	0.094	0.095	tbc	tbc	tbc	tbc
300-800m	-0.001	-0.002	0.029	0.033	tbc	tbc	tbc	tbc
800-2000m	0.000	0.000	0.011	0.013	tbc	tbc	tbc	tbc
2000-5000m	0.000	-0.004	0.006	0.007	tbc	tbc	tbc	tbc
0-5000m	-0.001	-0.001	0.051	0.051	tbc	tbc	tbc	tbc

Table 39: TPA RMS and average salinity misfits in psu (observation-model) with respect to the CORIOLIS in situ observations, in contiguous layers from 0 to 5000m.

III.10.3 SLA

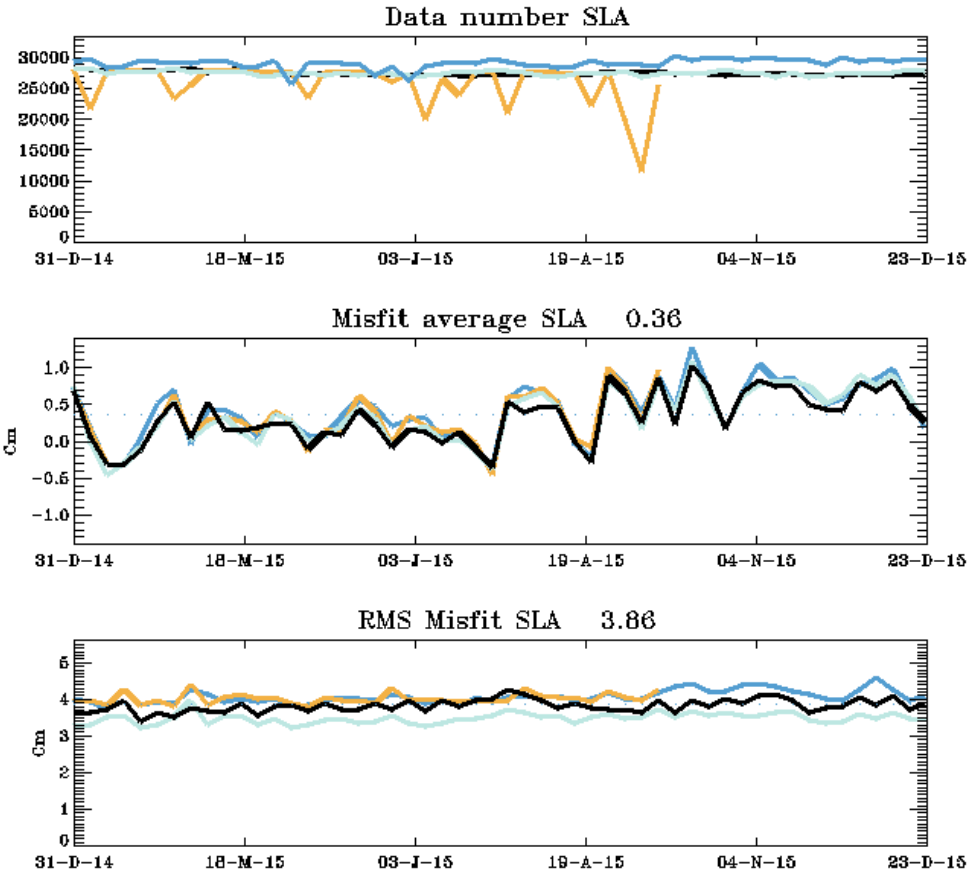

Figure 29: TPA RMS and average SLA misfits in cm (observation-model) with respect to all available altimetric missions in 2015 (black: Jason 2, cyan: SARAL/Altika, blue: HY-2, orange: Cryosat 2).

Seal Level Anomaly (cm)	Hindcast				Forecast			
	Mean misfit		RMS misfit		Mean misfit		RMS misfit	
	V2	V2.3	V2	V2.3	V2	V2.3	V2	V2.3
TPA	0.22	0.36	4.86	3.86	tbc	tbc	tbc	tbc

Table 40: TPA RMS and average SLA misfits in cm (observation-model) with respect to all available altimetric missions in 2015.

The SLA bias in the Tropical Pacific has increased by 0.1 cm in the V2.3 system, while the RMS has decreased by 1 cm, resulting in an overall improvement with respect to SLA in this region where the variability of SLA is closer to observations.

III.11 North Pacific Ocean NPA

III.11.1 Temperature

3D temperature accuracy results are synthesized in Table 41.

- Warm biases are found from the surface layer (0.06K) down to 800m (0.02K).
- RMS errors have slightly increased from V2 to V2.3 over the whole water column (<1K in the thermocline).

3DT (K)	Hindcast				Forecast day 3			
	Mean misfit		RMS misfit		Mean misfit		RMS misfit	
	V2	V2.3	V2	V2.3	V2	V2.3	V2	V2.3
0-5m	-0.02	-0.06	0.54	0.63	tbc	tbc	tbc	tbc
5-100m	0.02	-0.02	0.93	0.98	tbc	tbc	tbc	tbc
100-300m	-0.03	-0.03	0.77	0.83	tbc	tbc	tbc	tbc
300-800m	-0.01	-0.02	0.32	0.36	tbc	tbc	tbc	tbc
800-2000m	0.01	0.01	0.09	0.10	tbc	tbc	tbc	tbc
2000-5000m	0.01	0.04	0.05	0.07	tbc	tbc	tbc	tbc
0-5000m	0.00	0.00	0.36	0.39	tbc	tbc	tbc	tbc

Table 41: NPA RMS and average temperature misfits in K (observation-model) with respect to the CORIOLIS in situ observations, in contiguous layers from 0 to 5000m.

III.11.2 Salinity

3D salinity results are synthesized in Table 42.

- A fresh bias is found at the surface (0.015 psu) and biases close to zero are found in sub-surface (below 0.004 PSU).
- RMS error were reduced from V2 to V2.3 from the surface down to 300 m (<0.2 psu).
- Equivalent RMS errors under 300m or slight increase in V2.3 with respect to V2.

3DS(PSU)	Hindcast				Forecast day 3			
	RMS of misfit		Average misfit		RMS of misfit		Average misfit	
	V2	V2.3	V2	V2.3	V2	V2.3	V2	V2.3
0-5m	0.022	0.015	0.240	0.201	tbc	Tbc	tbc	tbc
5-100m	-0.004	0.003	0.184	0.168	tbc	Tbc	tbc	tbc
100-300m	-0.002	0.000	0.095	0.091	tbc	Tbc	tbc	tbc
300-800m	0.001	0.000	0.035	0.037	tbc	Tbc	tbc	tbc
800-2000m	0.001	0.001	0.013	0.014	tbc	Tbc	tbc	tbc
2000-5000m	0.003	0.001	0.008	0.009	tbc	Tbc	tbc	tbc
0-5000m	0.000	0.001	0.054	0.051	tbc	Tbc	tbc	tbc

Table 42: NPA RMS and average salinity misfits in psu (observation-model) with respect to the CORIOLIS in situ observations, in contiguous layers from 0 to 5000m.

III.11.3 SLA

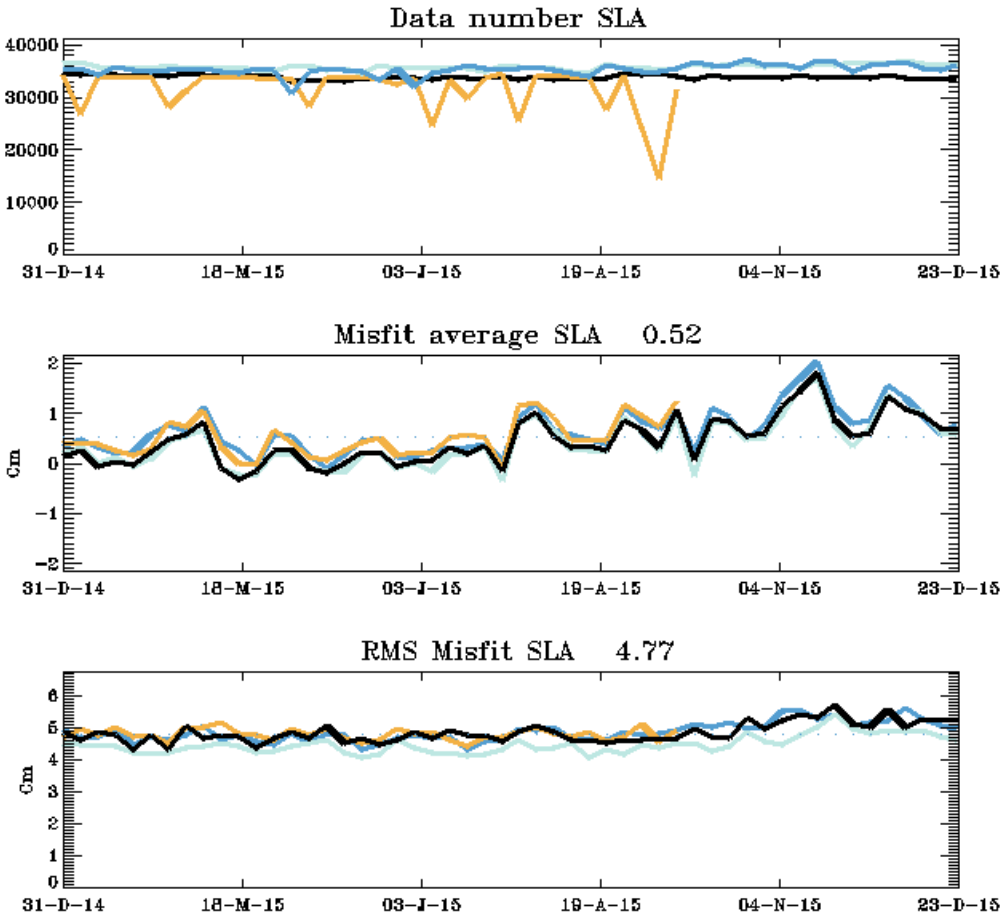

Figure 30: NPA RMS and average SLA misfits in cm (observation-model) with respect to all available altimetric missions in 2015 (black: Jason 2, cyan: SARAL/Altika, blue: HY-2, orange: Cryosat 2).

Seal Level Anomaly (cm)	Hindcast				Forecast day 3			
	Mean misfit		RMS misfit		Mean misfit		RMS misfit	
	V2	V2.3	V2	V2.3	V2	V2.3	V2	V2.3
NPA	0.25	0.52	5.63	4.77	tbc	tbc	tbc	tbc

Table 43: NPA RMS and average SLA misfits in cm (observation-model) with respect to Jason 1, Jason 2 and Envisat observations.

The SLA bias in the North Pacific has increased by 0.3 cm in the V2.3 system, while the RMS has decreased by 1 cm, resulting in an overall improvement with respect to SLA in this region where the variability of SLA is closer to observations.

IV QUALITY CHANGES SINCE PREVIOUS VERSION

This document focuses on the V2.3 version and analyses the quality changes with respect to V2. In consequence, quality changes since previous versions are synthesized in the executive summary.

V REFERENCES

Adcroft, A., Hill, C. and Marshall, J.: Representation of topography by shaved cells in a height coordinate ocean model, Mon. Weather Rev., 125, 2293-2315, 1997.

Amante C. and Eakins, B. W.: ETOPO1 1 Arc-minute global relief model: procedures, data sources and analysis, NOAA Technical Memorandum NESDIS NGDC-24, 25 pp., 2009.

Arakawa, A. and Lamb, V. R.: A potential enstrophy and energy conserving scheme for the shallow water equations, Mon. Weather. Rev.,109,18-36,1981.

Barnier, B., Madec, G., Penduff, T., Molines, J. M., Treguier, A. M., Le Sommer, J., Beckmann, A., Biastoch, A., Böning, C., Dengg, J., Derval, C., Durand, E., Gulev, S., Remy, E., Talandier, C., Theetten, S., Maltrud, M., McClean, J., and De Cuevas, B.: Impact of partial steps and momentum advection schemes in a global circulation model at eddy permitting resolution, Ocean Dynam., 56, 543-567, 2006.

Becker, J. J., Sandwell, D. T., Smith, W. H. F., Braud, J., Binder, B., Depner, J., Fabre, D., Factor, J., Ingalls, S., Kim, S.H., Ladner, R., Marks, K., Nelson, S., Pharaoh, A., Trimmer, R., Von Rosenberg, J., Wallace, G., and Weatherall, P.: Global Bathymetry and Elevation Data at 30 Arc Seconds Resolution: SRTM30_PLUS, Mar. Geod., 32, 355-371, doi: 10.1080/01490410903297766, 2009.

Benkiran, M. and Greiner, E.: Impact of the Incremental Analysis Updates on a Real-Time System of the North Atlantic Ocean, J. Atmos. Ocean. Tech., 25, 2055-2073, 2008.

Blanke, B. and Delecluse, P.: Variability of the tropical Atlantic-Ocean simulated by a general-circulation model with 2 different mixed-layer physics, J. Phys. Oceanogr., 23, 1363-1388, 1993.

Bloom, S. C., Takas, L. L., Da Silva, A. M., and Ledvina, D.: Data assimilation using incremental analysis updates, Mon. Weather Rev., 124, 1256-1271, 1996.

Brasseur, P. and Verron, J.: The SEEK filter method for data assimilation in oceanography: a synthesis. Ocean Dynamics.56 (5): 650-661, 2006.

Chambers, D.P., Cazenave, A., Champollion, N., Dieng, H., Llovel, W., Forsberg, R., Von Schuckmann, K. and Wada, Y.: Evaluation of the global mean sea level budget between 1993 and 2014. Surv. Geophys., early on-line, doi:10.1007/s10712-016-9381-3, 2016.

Chen, J. L., Wilson, C. R., Tapley, B. D., Famiglietti, J. S., and Rodell, M.: Seasonal global mean sea level change from satellite altimeter, GRACE, and geophysical models, J. Geodesy, 79, 532-539, doi:10.1007/s00190-005-0005-9, 2005.

Cravatte, S., Madec, G., Izumo, T., Menkes, C., and Bozec, A.: Progress in the 3-D circulation of the eastern equatorial Pacific in a climate, Ocean Model., 17, 28-48, 2007.

Dai, A. and Trenberth, K. E.: Estimates of freshwater discharge from continents: latitudinal and seasonal variations, J. Hydrometeorol., 3, 660–687, 2002.

Dai, A., Qian, T., Trenberth K. E. and Milliman J. D.: Changes in continental freshwater discharge from 1948-2004. J. Climate, 22, 2773-2791, 2009.

Desroziers, G., Berre, L., Chapnik, B., Poli, P.: Diagnosis of observation, background and analysis-error statistics in observation space, Q. J. R. Meteorol. Soc., 131: 3385-3396, 2005.

Fichefet, T. and Maqueda, M. A.: Sensitivity of a global sea ice model to the treatment of ice thermodynamics and dynamics, J. Geophys. Res., 102,12609-12646,1997.

Greatbatch, R.J.: A note on the representation of steric sea level in models that conserve volume rather than mass, J. Geophys. Res. Oceans 99 (C6), 12767–12771, http://dx.doi.org/10.1029/94JC00847, 1994.

Grodsky, S. A., Lumpkin, R., and Carton, J. A.: Spurious trends in global surface drifter currents, Geophys. Res. Lett., 38, L10606, doi: 10.1029/2011GL047393, 2011.

Huang, X. Y., Mogensen, K. S., and Yang, X.: First-guess at appropriate time: the HIRLAM implementation and experiments, Proc. HIRLAM Workshop on Variational Data Assimilation and Remote Sensing, Helsinki, Finland, Finnish Meteorological Institute, 28-43, 2002.

Hunke, E. C. and Dukowicz J. K.: An elastic-viscous-plastic model for sea ice dynamics, J. Phys. Oceanogr., 27, 1849-1867, 1997.

Koch-Larrouy, A., Madec, G., Blanke, B. and Molcard, R.: Water mass transformation along the Indonesian throughflow in an OGCM, Ocean Dynam., 58, 289-309, doi:10.1007/s10236-008-0155-4, 2008.

Large, W. G. and Yeager, S. G.: The global climatology of an interannually varying air–sea flux data set, Clim. Dynam., 33, 341-364, doi:10.1007/s00382-008-0441-3, 2009.

Lellouche, J.-M., Le Galloudec, O., Drévillon, M., Régnier, C., Greiner, E., Garric, G., Ferry, N., Desportes, C., Testut, C.-E., Bricaud, C., Bourdallé-Badie, R., Tranchant, B., Benkiran, M., Drillet, Y., Daudin, A., and De Nicola, C.: Evaluation of global monitoring and forecasting systems at Mercator Océan, Ocean Sci., 9, 57-81, 2013.Lévy, M., Estublier, A., and Madec, G.: Choice of an advection scheme for biogeochemical models, Geophys. Res. Lett., 28, 3725–3728, doi:10.1029/2001GL012947, 2001.

Locarnini, R. A., A. V. Mishonov, J. I. Antonov, T. P. Boyer, H. E. Garcia, O. K. Baranova, M. M. Zweng, C. R. Paver, J. R. Reagan, D. R. Johnson, M. Hamilton, and D. Seidov, 2013. World Ocean Atlas 2013, Volume 1: Temperature. S. Levitus, Ed., A. Mishonov Technical Ed.; NOAA Atlas NESDIS 73, 40 pp.

Madec, G. and Imbard M.: A global ocean mesh to overcome the North Pole singularity, Clim. Dynam., 12, 381-388, 1996.

Madec, G. and the NEMO team: NEMO ocean engine. Note du Pôle de modélisation, Institut Pierre-Simon Laplace (IPSL), France, No. 27 ISSN, 1288-1619, 2008.

Oke, P. R., Brassington, G. B., Griffin, D. A., and Schiller, A.: The Bluelink Ocean Data Assimilation System (BODAS), Ocean Model., 21, 46-70, 2008.

Rio, M. H., Guinehut, S., and Larnicol, G.: New CNES-CLS09 global mean dynamic topography computed from the combination of GRACE data, altimetry, and in situ measurements, J. Geophys. Res., 116, C07018, doi:10.1029/2010JC006505, 2011.

Rio, M.-H., Mulet, S. and Picot, N.: Beyond GOCE for the ocean circulation estimate: Synergetic use of altimetry, gravimetry, and in situ data provides new insight into geostrophic and Ekman currents, Geophys. Res. Lett., 41, doi:10.1002/2014GL061773, 2014.

Roquet, F., Charrassin, J. B., Marchand, S., Boehme, L., Fedak, M., Reverdin, G., and Guinet, C.: Delayed-mode calibration of hydrographic data obtained from animal-borne satellite relay data loggers, J. Atmos. Ocean. Tech., 28, 787–801, 2011.

Roullet, G. and Madec, G.: Salt conservation, free surface, and varying levels: a new formulation for ocean general circulation models, J. Geophys. Res., 105, 23927–23942, 2000.

St.Laurent, L.C., Simmons, H.L., Jayne, S.R. : Estimating tidally driven mixing in the deep ocen, Geophys. Res. Lett. 29, 2106, 10.1029/2002GL015 633, 2002.

Silva, T. A. M., Bigg, G. R., and Nicholls, K. W.: Contribution of giant icebergs to the Southern Ocean freshwater flux, J. Geophys. Res., 111, C03004, doi:10.1029/2004JC002843, 2006.

Tournadre, J., F. Accensi, F. and Girard-Ardhuin, F.: The ALTIBERG iceberg database, Doc. Tech. LOS 2013-01, Ver. 1.0, Ifremer, Plouzan, France, Available at ftp://ftp.ifremer.fr/ifremer/cersat/projects/altiberg, 2013.

Tranchant, B., Reffray, G., Greiner, E., Nugroho, D., Koch-Larrouy, A. and Gaspar, P.: Evaluation of an operational ocean model configuration at 1/12° spatial resolution for the Indonesian seas (NEMO2.3/INDO12) – Part 1: Ocean physics, Geosci. Model Dev., 9, 1037-1064, 2016.

Zweng, M.M, J.R. Reagan, J.I. Antonov, R.A. Locarnini, A.V. Mishonov, T.P. Boyer, H.E. Garcia, O.K. Baranova, D.R. Johnson, D.Seidov, M.M. Biddle: World Ocean Atlas 2013, Volume 2: Salinity. S. Levitus, Ed., A. Mishonov Technical Ed.; NOAA Atlas NESDIS 74, 39 pp., 2013.

VI APPENDIX

VI.1 GODAE Regions

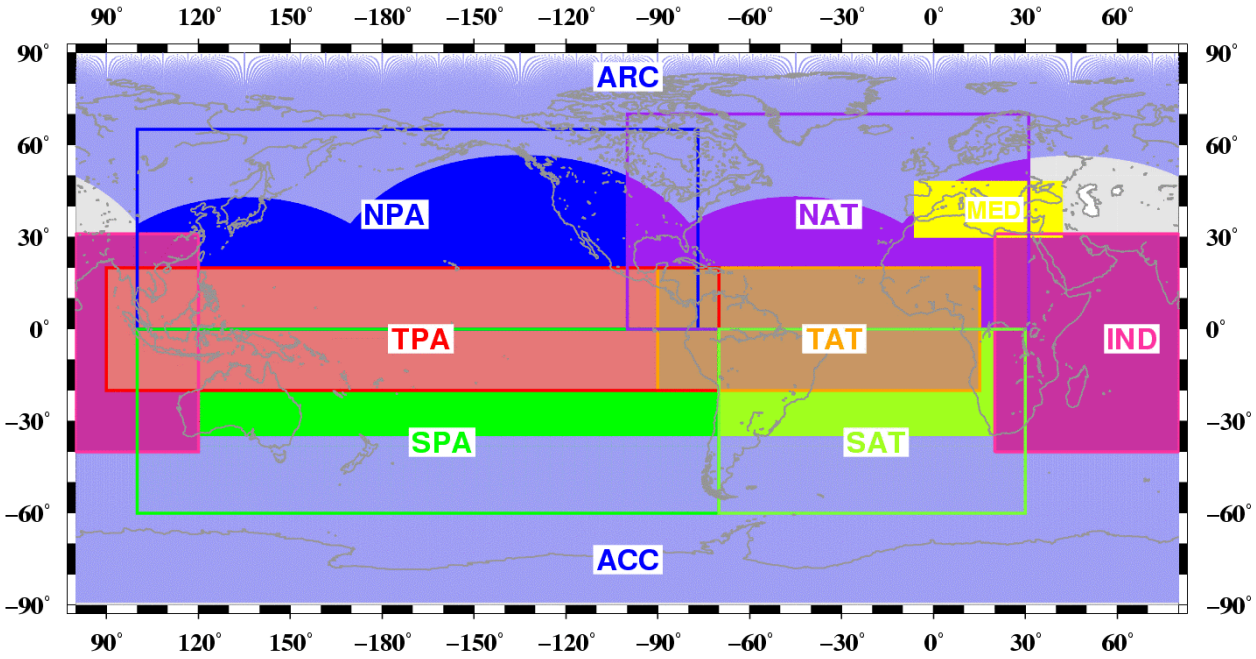

Figure 31: The regional description of GODAE regions

VI.2 Data assimilation glossary

Misfit	Difference between the observation and its model counterpart at the time and location of the observation. The model counterpart is possibly transformed to be compared to the observation

	(filtered in space and time, for instance)
Innovation	Same as misfit
forecast	In the data assimilation context it's the name given to the model counterpart for the misfit computation (model value before any correction)
background	Same as forecast
guess	Same as forecast
analysis	Model forecast (or guess) corrected with the increment (or correction)
Residual	Difference between the observation and its analysis counterpart at the time and location of the observation.
hindcast	Numerical experiment describing a period in the past.